

UNCLASSIFIED

AD NUMBER

AD484822

LIMITATION CHANGES

TO:

Approved for public release; distribution is unlimited.

FROM:

Distribution authorized to U.S. Gov't. agencies and their contractors; Critical Technology; JUN 1966. Other requests shall be referred to Arnold Engineering Development Center, Arnold AFS, TN. This document contains export-controlled technical data.

AUTHORITY

AEDC ltr , 15 Jun 1973

THIS PAGE IS UNCLASSIFIED

AEDC-TR-66-125

ARCHIVE COPY
DO NOT LOAN



TRANSONIC STATIC AND DYNAMIC STABILITY
CHARACTERISTICS OF SEVERAL SATURN IB
AND V UPPER STAGE CONFIGURATIONS

R. I. Lowndes and T. O. Shadow
ARO, Inc.

This document is not loan approved for public release
and distribution is controlled. For A. G. Letter
dated 15 Jan 73

June 1966 PROPERTY OF U. S. AIR FORCE
AEDC LIBRARY
AF 40(600)1200

This document is subject to special export controls
and each transmittal to foreign governments or foreign
nationals may be made only with prior approval of
NASA-MSFC

PROPELLION WIND TUNNEL FACILITY
ARNOLD ENGINEERING DEVELOPMENT CENTER
AIR FORCE SYSTEMS COMMAND
ARNOLD AIR FORCE STATION, TENNESSEE

AEDC TECHNICAL LIBRARY

5 0720 00031 3340

NOTICES

When U. S. Government drawings, specifications, or other data are used for any purpose other than a definitely related Government procurement operation, the Government thereby incurs no responsibility nor any obligation whatsoever, and the fact that the Government may have formulated, furnished, or in any way supplied the said drawings, specifications, or other data, is not to be regarded by implication or otherwise, or in any manner licensing the holder or any other person or corporation, or conveying any rights or permission to manufacture, use, or sell any patented invention that may in any way be related thereto.

Qualified users may obtain copies of this report from the Defense Documentation Center.

References to named commercial products in this report are not to be considered in any sense as an endorsement of the product by the United States Air Force or the Government.

TRANSonic STATIC AND DYNAMIC STABILITY
CHARACTERISTICS OF SEVERAL SATURN IB
AND V UPPER STAGE CONFIGURATIONS

R. I. Lowndes and T. O. Shadow
ARO, Inc.

This document is subject to special export controls
and each transmittal to foreign governments or foreign
nationals may be made only with prior approval of
NASA-MSFC.

This document has been approved for public release
as its distribution is unlimited. *Per A. A. letter*
dated 15 June, 1973

FOREWORD

The work reported was done as the result of a joint request by the National Aeronautics and Space Administration (NASA), Marshall Space Flight Center (MSFC), and the Lockheed Missiles and Space Company, Huntsville Research and Engineering Center (LMSC/MSFC), under System 921E.

The tests were conducted by ARO, Inc. (a subsidiary of Sverdrup & Parcel and Associates, Inc.), contract operator of the Arnold Engineering Development Center (AEDC), Air Force Systems Command (AFSC), Arnold Air Force Station, Tennessee, under Contract AF40(600)-1200. The tests were conducted from August 26, 1965, to March 14, 1966, under ARO Project Number PA1514, and the manuscript was submitted for publication on June 3, 1966.

This technical report has been reviewed and is approved.

Theodore E. Workman
Major, USAF
AF Representative, PWT
DCS/Test

Leonard T. Glaser
Colonel, USAF
DCS/Test

ABSTRACT

Dynamic stability characteristics of six Apollo-Saturn IB and V and one Saturn-Centaur upper stage model configurations and static stability characteristics of two Apollo-Saturn IB and V upper stage model configurations were obtained from $M_\infty = 0.50$ to 1.40. The primary test objective was to investigate the changes in dynamic stability characteristics as a function of pitch oscillation center. A secondary objective was to compare three different model mounting techniques - sting, transverse rod, and reflection plane. The static testing resulted from a suspected nonlinear phenomenon observed during the dynamic phase of the test. One model configuration which was stable when the pitch oscillation center was ahead of a separation disk exhibited limit cycle oscillations when the pitch oscillation center was located aft of the disk.

CONTENTS

	<u>Page</u>
ABSTRACT	iii
NOMENCLATURE	vii
I. INTRODUCTION	1
II. APPARATUS	
2.1 Test Facility	2
2.2 Test Article	2
III. TEST DESCRIPTION	
3.1 Procedure	2
3.2 Data Reduction	3
3.3 Precision of Measurements.	3
IV. RESULTS AND DISCUSSION	
4.1 Variation of Pitch Oscillation Center	5
4.2 Results of Different Mounting Techniques	6
4.3 Static Test Results	7
V. CONCLUSIONS AND RECOMMENDATIONS	7
REFERENCES	11
APPENDIX: Data Reduction Equations	9

ILLUSTRATIONS

Figure

1. Schematic of Model Installation in Tunnel 1T	
a. Sting-Mounted Model	13
b. Transverse Rod-Supported Model	14
2. Photographs showing Typical Model Installation and Rotation Centers	
a. Configuration B ₁ DS ₁ -05S, Sting Mounted	15
b. Configuration B ₁ S ₁ -02R, Transverse Rod Supported	16
c. Configuration B ₁ -01P, Reflection Plane Mounted.	17
d. Three Model Rotation Centers, 01, 02, and 05	18
e. Transverse Rod and Reflection Plane Mounting of the B ₁ -01 Configuration	19
3. Model Configuration Drawings	
a. Configuration B ₁ -01 (B ₁ D-01)	20
b. Configuration B ₁ -02 (B ₁ D-02)	21

<u>Figure</u>	<u>Page</u>
3. Continued	
c. Configuration B ₁ S ₁ -05 (B ₁ DS ₁ -05, B ₁ CS ₁ -05)	22
d. Configuration B ₁ -01P	23
e. Details of B ₁ Command Module and Escape Rocket.	24
f. Details of Rocket Tower.	25
g. Configuration CR-I and CR-II	26
4. Reynolds Number Variation with Mach Number	27
5. Apollo-Saturn Model Configurations; Effect of Pitch Oscillation Center on Dynamic Stability Derivatives versus Mach Number, $\alpha = 0$	
a. Configuration B ₁	28
b. Configuration B ₁ D	28
c. Configuration B ₁ S ₁	29
d. Configuration B ₁ DS ₁	29
6. Saturn-Centaur Model Configurations; Effect of Pitch Oscillation Center on Stability Derivatives versus Mach Number, $\alpha = 0$, Configurations CR-IIS and CR-IIIS	30
7. Saturn-Centaur Model Configuration; Stability Derivatives versus Angle of Attack, $M_\infty = 0.70$, 0.90 , and 0.95 , Configuration CR-IIIS	31
8. Dynamic Stability Derivatives versus Mach Number Compared for Different Model Mounting Techniques, $\alpha = 0$	
a. Configuration B ₁ S ₁ -05.	32
b. Configuration B ₁ DS ₁ -05	32
c. Configuration B ₁ -01.	33
9. Apollo-Saturn Stability Derivatives versus Mach Number, Configurations B ₁ S ₁ -05S and B ₁ CS-05S, $\alpha = 0$	34
10. Static Force and Moment Coefficients for Apollo-Saturn Configurations B ₁ S ₁ -05S and B ₁ DS ₁ -05S	
a. Configuration B ₁ S ₁ -05S	35
b. Configuration B ₁ DS ₁ -05S	36
11. Static Stability Derivatives for Apollo-Saturn Configurations B ₁ S ₁ -05S and B ₁ DS ₁ -05S	
a. Configuration B ₁ S ₁ -05S	37
b. Configuration B ₁ DS ₁ -05S	37

TABLE

	<u>Page</u>
--	-------------

NOMENCLATURE

A	Base area of model (reference area), 0.1226 ft ²
d	Base diameter of model (reference length), 0.125 ft
C _A	Axial-force coefficient, measured axial force/ $q_{\infty} A$
C _m	Pitching-moment coefficient, pitching moment/ $q_{\infty} A d$
C _{mα}	Rate of change of pitching-moment coefficient with angle of attack, $dC_m/d\alpha$, per rad
C _{m$\dot{\theta}$} + C _{m$\dot{\alpha}$}	Effective value of dynamic stability parameter (see Appendix), per rad
C _N	Normal-force coefficient, normal force/ $q_{\infty} A$
M _{∞}	Free-stream Mach number
P _t	Total pressure, psf
p _{∞}	Free-stream static pressure, psf
q _{∞}	Free-stream dynamic pressure, 0.7 p _{∞} M _{∞} ² , psf
Re/ft	Reynolds number/ft, V _{∞} / ν_{∞}
T	Temperature, °R
t	Time, sec
V _{∞}	Free-stream velocity, ft/sec
α	(i) Mean angle of attack about which oscillations occur. (ii) Angle of attack, deg
$\dot{\alpha} = \frac{d\alpha}{dt}$	Time rate of change of angle of attack, rad/sec
θ	Instantaneous pitch angle measured relative to the mean angle of attack ($\theta = \bar{\theta} \sin \omega t$), deg
$\bar{\theta}$	(i) Pitch oscillation amplitude. (ii) Pitch oscillation amplitude of limit cycle oscillations, deg

$\dot{\theta} = \frac{d\theta}{dt}$ Time rate of change of instantaneous pitch angle, rad/sec

ν_∞ Free-stream kinematic viscosity, ft²/sec

ω Circular frequency, rad/sec

SUBSCRIPT

t Total

SECTION I INTRODUCTION

This report presents the rigid body dynamic and static stability characteristics of several upper stage model configurations of the Saturn IB and V space vehicle. The data were obtained in the Aerodynamic Wind Tunnel, Transonic (1T).

The primary test objective was to measure the model stability as a function of pitch oscillation center in the transonic Mach number range from 0.50 to 1.40. This test objective resulted from an analytical study (Ref. 1) which predicted the possibility of statically stabilizing loads becoming dynamically destabilizing when the pitch oscillation center is located between the origin of a separated flow field and an afterbody submerged in the separated flow.

A secondary test objective was to compare three different model mounting techniques - sting, transverse rod, and reflection plane. The transverse rod supporting technique resulted from the requirement to oscillate the models over a wide range of pitch oscillation centers. This mounting technique appeared to be the more efficient. The reflection plane mounting was employed more for academic purposes of correlation than a principal method of obtaining data. The sting-mounting technique was employed both in the dynamic and static phases of the test. The intended purpose of the sting-mount dynamic test was to investigate the transverse rod effect on dynamic stability. During the course of the dynamic sting-mount phase of the test, two configurations were observed to oscillate about a nonzero angle of attack when the sting was at zero pitch angle. Consequently, a sting-mount, static force and moment investigation was conducted to determine possible pitching-moment nonlinearities with angle of attack.

The tests were conducted in two separate tunnel entries. During the first entry three Apollo-Saturn IB and V upper stage and two Saturn-Centaur model configurations were tested on a sting-mounted, free-pitch, oscillation balance. During the second entry, four Apollo-Saturn IB and V upper stage model configurations were tested on a sting-mounted static-force balance. One half-model configuration mounted on a reflection plane was tested in free-pitch oscillation. Comparison of test results for the three mounting techniques is presented in the report.

SECTION II APPARATUS

2.1 TEST FACILITY

The tests were conducted in Tunnel 1T. A description of the tunnel and associated equipment can be found in Ref. 2.

Schematics of the test section with sting-mounted and transverse rod mounted models are presented in Figs. 1a and b, respectively. Photographs of typical model installations are presented in Fig. 2.

2.2 TEST ARTICLE

Six Apollo-Saturn IB and V upper stage model configurations were tested in free-pitch oscillation. Two of the six configurations were tested statically. In addition, two model configurations of the Saturn-Centaur upper stage were tested in free-pitch oscillation. Model configuration descriptions are presented in Table I, and basic model configuration drawings are shown in Fig. 3. All Apollo-Saturn IB and V upper stage model configurations included the escape rocket and tower.

The reflection plane model configuration (Fig. 3d) has one significant distinguishing feature from most other dynamic reflection plane models. The half-model is spaced away from but attached integral with the reflection plane disk. It was reasoned that viscous "clutch" damping would be measured along with aerodynamic damping if the half-model were permitted to oscillate relative to the disk. This type of damping could possibly obscure the small aerodynamic damping values.

A description of the wall-mounted, free-pitch oscillation, transverse rod balance can be found in Ref. 3. A description of the basic sting-mounted, free-pitch oscillation balance can be found in Ref. 2.

SECTION III TEST DESCRIPTION

3.1 PROCEDURE

3.1.1 Sting-Mounted Balances

Both a free-pitch oscillation and static-force balance were employed. In the case of free oscillation testing, the model amplitude was obtained

by alternate air pulses impinging on the rear "skirt" of the model. After a desired steady-state oscillatory amplitude was obtained, the air jet system was valved closed and the subsequent transient oscillations recorded. Static-force and moment data were obtained by pitching the model from -2- to 5-deg angle of attack. A three-component, static-force balance was used. Base pressure measurements were not obtained.

3.1.2 Wall-Mounted, Transverse Rod Balance

A mechanical cocking device provided the means by which the models could be released from angle of attack. The models were usually released from a 4.5-deg amplitude and the subsequent oscillations recorded.

3.1.3 Wall-Mounted, Reflection Plane Balance

The reflection plane model was tested on the wall-mounted, transverse rod balance by suitably modifying the model attachment point, as shown in Fig. 3d.

3.1.4 General Test Conditions

Data were obtained at $M_\infty = 0.50, 0.60, 0.70, 0.80, 0.90, 0.95, 1.00, 1.05, 1.10$, and 1.40 . The tunnel total pressure, which varies with ambient pressure and temperature, ranged from 2755 to 2887 psf. The variation of Reynolds number with Mach number is presented in Fig. 4.

3.2 DATA REDUCTION

The free-pitch oscillation data reduction equations are presented in the Appendix. Except where limit cycle amplitudes exceeded ± 2 deg, the damping derivatives, $Cm_{\dot{\theta}} + Cm_{\ddot{\theta}}$, presented corresponded to the number of cycles to half amplitude over the oscillation amplitude range from ± 4 to ± 2 deg. Where limit cycle amplitudes were involved, and did not exceed ± 3 deg, the decrement measurements were obtained between ± 4 and ± 3 deg. No decrement measurements were obtained when the limit cycle amplitude exceeded ± 3 deg.

3.3 PRECISION OF MEASUREMENTS

The estimated precision of the data obtained during the investigation is as follows:

<u>Quantity</u>	<u>Uncertainty</u>
α static	± 0.10 deg
α dynamic	± 0.20 deg
p_t	± 3 psf
M_∞	± 0.008
T_t	$\pm 2^\circ R$
C_A	± 0.008
C_m	± 0.002
$C_{m\alpha}$	± 0.090
$C_{m\dot{\theta}} + C_{m\dot{\alpha}}$	± 1.00
C_N	± 0.01
$\omega/2\pi$	± 2 cps

The above uncertainties are based on inaccuracies in balance, oscillograph, and pressure transducer measurements. The streamwise variation of M_∞ in the vicinity of the model probably did not exceed ± 0.003 at $M_\infty = 0.7$ (Ref. 4) and ± 0.015 at $M_\infty = 1.40$.

SECTION IV RESULTS AND DISCUSSION

The test results are presented in a form, Figs. 5 and 6, that illustrates the effect of pitch oscillation center on the dynamic stability. Stability derivatives as a function of angle of attack for one Saturn-Centaur model configuration are presented in Fig. 7 for $M_\infty = 0.70$, 0.90, and 0.95. The dynamic stability results obtained for certain model configurations mounted on the sting-supported balance, the transverse rod balance, and the reflection plane mounting are presented in Fig. 8. Stability derivatives for two Apollo-Saturn, sting-mounted configurations are presented in Fig. 9. In Fig. 10, sting-mount static-force and moment results are presented. Static stability derivatives obtained from the sting-mounted, free-pitch oscillation balance are compared with the corresponding results from the static data in Fig. 11.

No quantitative static stability results were obtained from the transverse rod, free oscillation balance. The mechanical stiffness of the balance was several orders of magnitude greater than the aerodynamic

stiffness. Consequently, small changes in aerodynamic stiffness produced no measurable differences in frequency. Qualitatively, however, the static stability increased as the model pitch oscillation center was moved from rear to front.

Statically unstable models could be tested dynamically because of an overall balance system stability.

4.1 VARIATION OF PITCH OSCILLATION CENTER

The various pitch oscillation centers (see Fig. 3) were coincident with structural bending nodal points for the entire Apollo-Saturn IB and V space vehicle (Ref. 1). It seemed reasonable that the upper stage aerodynamic stability contribution to the entire vehicle could be obtained from pitch oscillation tests where oscillation centers correspond to nodal points. From Fig. 3a it can be observed that the 01 pitch oscillation center passes through the escape rocket ahead of the separation disk, D. The 02 pitch oscillation center (Fig. 3b) passed through the escape rocket tower and just downstream of the disk. The 05 pitch oscillation center (Fig. 3c) passed through the junction between the B₁ command module and the skirt S₁, also downstream of the disk, but farther aft of the 02 pitch oscillation center.

From Ref. 1, an analytical study of the quasi-steady transonic flow characteristics predicted that statically stabilizing loads could become dynamically destabilizing when a nodal point (pitch oscillation center) was between a separation source (D) and an afterbody (B₁, B₁S₁) immersed in the separated flow field. A phase shift could arise because of the time lag between the instant the separation source was perturbed and the instant the separated flow field altered the submerged body loads, thus causing instability.

Unfortunately, a single model configuration could not be tested at all three pitch oscillation centers - 01, 02, and 05 - because of structural requirements for the models. For example, tests of a B₁S₁-01 configuration were prohibited because inertia loads of the B₁S₁ portion of the model could have caused structural failure of the tower at the testing frequency of from 53 to 55 cps.

For model configuration B₁ (Table I), Fig. 5a shows that shifting the pitch oscillation center from the 01 position to the 02 position had a destabilizing effect. As shown in Fig. 5b, the addition of the disk at the base of the escape rocket (Fig. 3a) produced limit cycle oscillations throughout the Mach number range for the 02 pitch oscillation center. When the pitch

oscillation center was located at the 01 position, the limit cycle oscillations occurred only below Mach number 0.8.

In Figs. 5c and d comparison of the 02 and 05 pitch oscillation center results for configurations B₁S₁ and B₁DS₁ are presented. Figure 5c shows that above $M_\infty = 0.6$ a shift from the 02 to 05 pitch oscillation center corresponded to a decrease in stability for the B₁S₁ configuration. Similarly, for the B₁DS₁ configuration (Fig. 5d), greater stability was observed for the 02 position.

Summarizing the results of Figs. 5a through 5d, an increase in static stability was accompanied by a corresponding increase in dynamic stability. To be entirely consistent with the arguments of Ref. 1, the dynamic stability level for the 02 position should be lower than either the 01 or 05 level. It is possible, however, that the S₁ skirt was not fully immersed in the separated flow field, and as a result, any destabilizing loads acting on the B₁ module were obscured. The stability trend from the 01 to 02 pitch oscillation center was consistent with that reported in Ref. 1.

In Fig. 6 the stability characteristics of two Saturn-Centaur upper stage configurations, CR-IS and CR-IIS, are presented. The results in Fig. 6 showed little change in the dynamic stability parameter as the pitch oscillation center was shifted from the II to the I position (Fig. 3g).

In Figs. 7 values of $C_{m\dot{\theta}} + C_{m\dot{\alpha}}$ for $M_\infty = 0.70$, 0.90, and 0.95 are presented as a function of mean angle of attack, α , for the CR-II configuration. This figure is significant in that it shows a greater variation at small angles of attack rather than at large angles of attack.

4.2 RESULTS OF DIFFERENT MOUNTING TECHNIQUES

Three model mounting techniques were employed: sting, transverse rod, and reflection plane. However, no single configuration was tested with all three techniques. In Figs. 8a and b, $C_{m\dot{\theta}} + C_{m\dot{\alpha}}$ values for configurations B₁S₁ and B₁DS₁ at the 05 pitch oscillation center are compared for free oscillation sting and transverse rod supports. The comparison is conditional by the fact that the sting-mounted data were obtained in the frequency range from 28 to 32 cps whereas the rod supported data were obtained over the range from 53 to 56 cps. The quasi-steady theory of Ref. 1 is based upon the lag time between a separated and an attached flow impingement on an oscillating body. If this concept is correct, then some discrepancy between the rod and sting values of $C_{m\dot{\theta}} + C_{m\dot{\alpha}}$ in Fig. 8a and b might be explained as a frequency effect. This argument is partially supported by the agreement shown in Fig. 8c between the

rod and reflection plane results of the B₁-01 configuration. Here the frequency range was approximately the same (53 to 55 cps). The singular disagreement at $M_{\infty} = 1.10$ is unexplained. Unfortunately, little time was available for the reflection plane phase of testing.

A comparison of the stability derivatives of two sting-mounted configurations, B_{1S1}-05S and B_{1CS1}-05, is presented in Fig. 9. The center spike, C, (Fig. 3c) was representative of a free-flight model tower stiffener used in ballistic range tests. Apparently, there was only a slight increase in dynamic stability, at $M_{\infty} = 0.95$, attributable to the center spike.

4.3 STATIC TEST RESULTS

As mentioned earlier in the report, a static test was conducted to investigate a suspected nonlinear pitching-moment phenomenon associated with the B_{1S1}-05S and B_{1DS1}-05S configurations. During the dynamic phase of the sting-support testing, both the B_{1S1} and B_{1DS1} models were observed to oscillate about a sometimes unrepeatable and intermittent static trim angle, different from zero, in the Mach number range from 0.90 to 1.10. As shown in Figs. 10a and b, the sting-support, static-force and moment investigation apparently did not reveal any abrupt nonlinearities in C_N and C_m with angle of attack. The trim angle behavior appears to be the result of a simple static instability. A comparison of the static stability parameter, $C_{m_{\alpha}}$, as obtained from both static and dynamic sting-supported balances, is presented in Figs. 11a and b for configurations B_{1S1} and B_{1DS1}, respectively. The rather poor agreement might be the result of pressure lag in the dynamic case that is not present in the static case.

SECTION V CONCLUSIONS AND RECOMMENDATIONS

The effect of varying pitch oscillation center showed that the dynamic stability was altered. Whether the corresponding changes in $C_{m_{\dot{\theta}}} + C_{m_{\dot{\alpha}}}$ values were consistent with the quasi-steady arguments of Ref. 1 was not resolved.

No significant variations in the data are believed to have resulted from the three model mounting techniques employed: sting, transverse rod, and reflection plane.

The free-pitch oscillation testing technique did not provide a suitable means to study the nonlinear aerodynamic stability problem associated with the separated flow effects. Forced oscillation testing in which the aerodynamic damping torque is measured directly would afford more complete test results. High response pressure measurements on a larger scale model might shed some light on the time dependency of pressure lag in a separated flow field.

APPENDIX I
DATA REDUCTION EQUATIONS

The free-pitch oscillation, dynamic data reduction equations are

$$C_{m\dot{\theta}} + C_{m\dot{a}} = - \frac{80\sqrt{T_1} \left(1 + 0.2M_\infty^2\right)^3 I}{p_1 M_\infty^2 A d^2} \left\{ (\zeta\omega_0)_2 - (\zeta\omega_0)_1 \frac{\omega_1}{\omega_2} \right\}$$

$$C_{m\alpha} = 1.428 \frac{\left(1 + 0.2M_\infty^2\right)^{3.5} I}{p_1 M_\infty^2 A d} \left\{ (\omega_1^2 - \omega_2^2) + \left[(\zeta\omega_0)_1^2 - (\zeta\omega_0)_2^2 \right] \right\}$$

where

$$(\zeta\omega_0)_i = \frac{\omega_1}{n\pi} + \ln 2, \quad i = 1, 2$$

ω_0 = Natural circular frequency

ω_i = Resonant circular frequency

n = Number of cycles to 1/2 amplitude of $\bar{\theta}_j$

ζ = Critical damping ratio

Subscript Notations

1	Wind-off
2	Wind-on
o	Natural
j	Initial

MODEL CONSTANTS

$$A = 0.01226 \text{ ft}^2$$

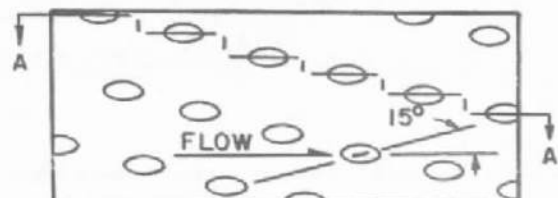
$$d = 0.125 \text{ ft}$$

Model Configuration	Model and Balance Inertia, ft-lb-sec ² x 10 ⁶
B ₁ -01R	606.5
B ₁ D-01R	606.5
B ₁ -02R	602.6

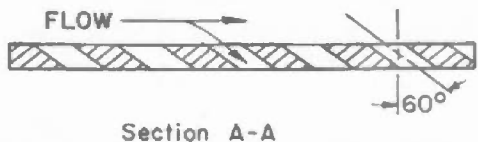
<u>Model Configuration</u>	<u>Model and Balance Inertia, ft-lb-sec² x 10⁶</u>
B ₁ D-02R	602.6
B ₁ S ₁ -02R	621.8
B ₁ DS ₁ -02R	621.8
B ₁ S ₁ -05R	615.3
B ₁ DS ₁ -05R	615.3
B ₁ DCS ₁ -05R	615.3
B ₁ -01P	695.3
Plate and Balance	681.9
B ₁ S ₁ -05S	22.7
B ₁ DS ₁ -05S	22.7
B ₁ CS ₁ -05S	22.7
CR-IS	51.8
CR-IIS	44.4

REFERENCES

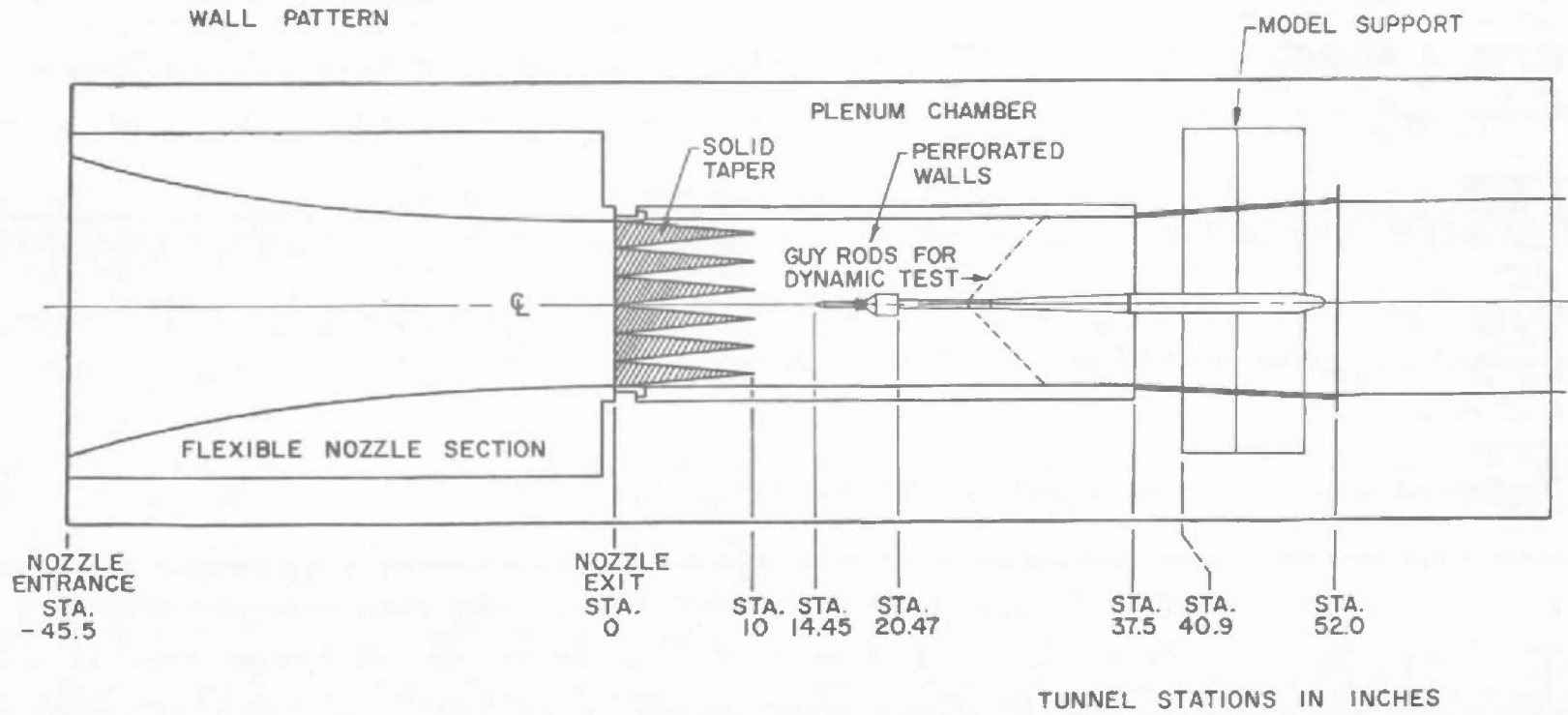
1. Ericson, Lars-Eric. "Report on Saturn I-Apollo Unsteady Aerodynamics." LMSC-A650215, February 1964.
2. Test Facilities Handbook (5th Edition). "Propulsion Wind Tunnel Facility, Vol. 3." Arnold Engineering Development Center, July 1963.
3. Lowndes, R. I. "Static and Dynamic Stability Characteristics of Several M and M Planform Wings at Transonic Speeds." AEDC-TDR-64-99 (AD440851), June 1964.
4. Nichols, J. H. and Jackson, F. M. "A Check Calibration of the AEDC-PWT Transonic Model Tunnel." AEDC-TDR-62-206 (AD287183), October 1962.



TYPICAL PERFORATED
WALL PATTERN



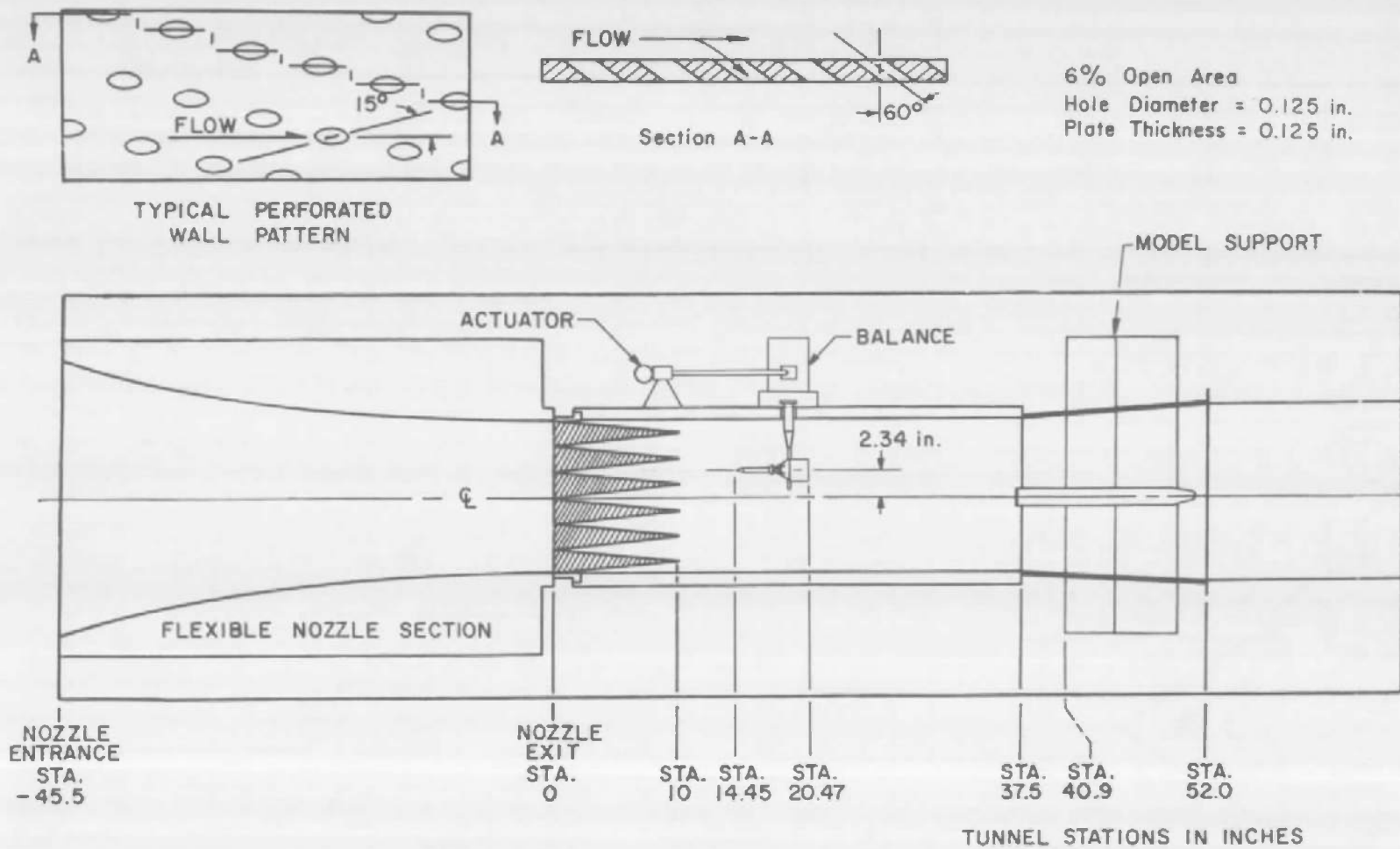
6% Open Area
Hole Diameter = 0.125 in.
Plate Thickness = 0.125 in.



TUNNEL STATIONS IN INCHES

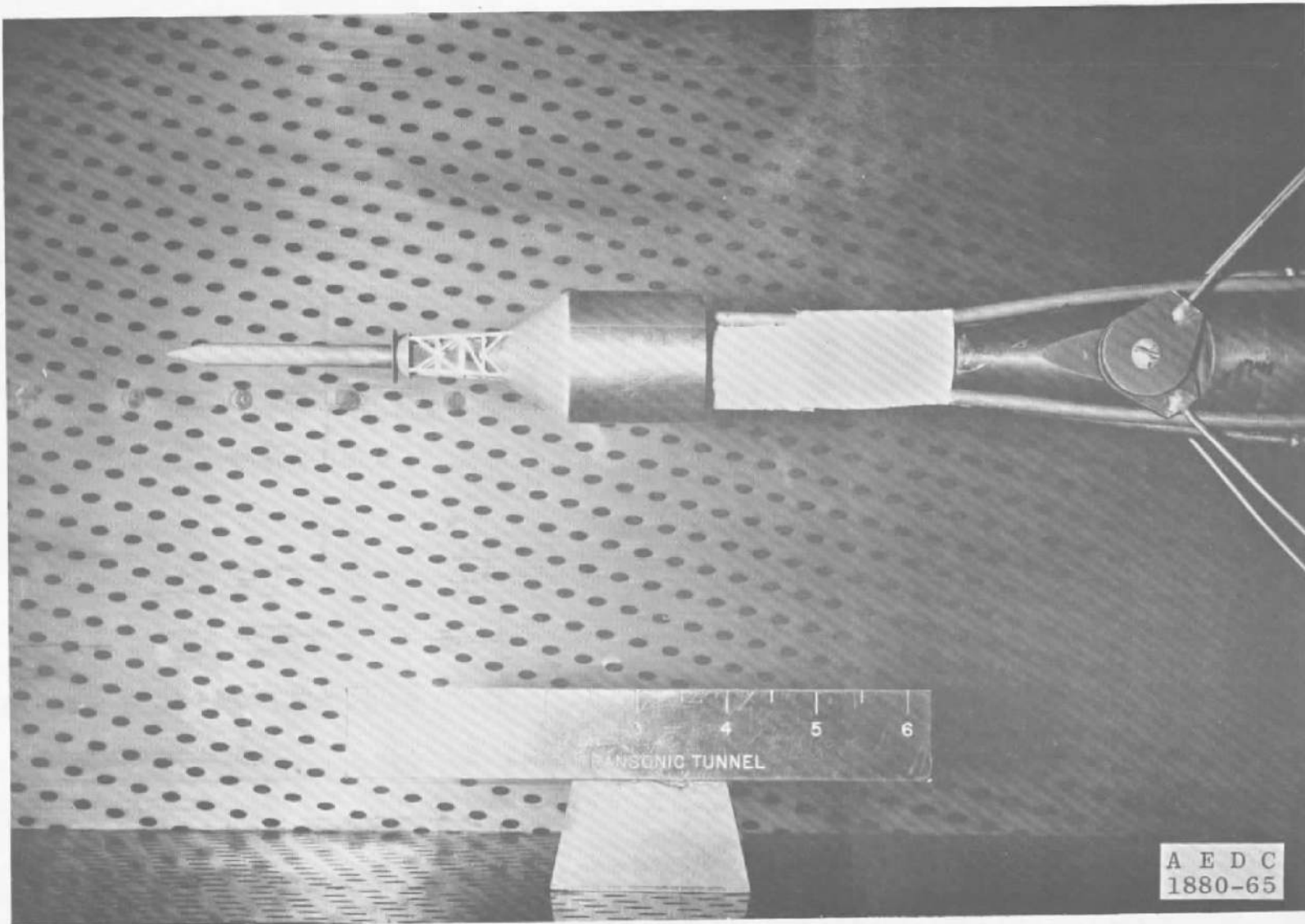
o. Sting-Mounted Model

Fig. 1 Schematic of Model Installation in Tunnel 1T

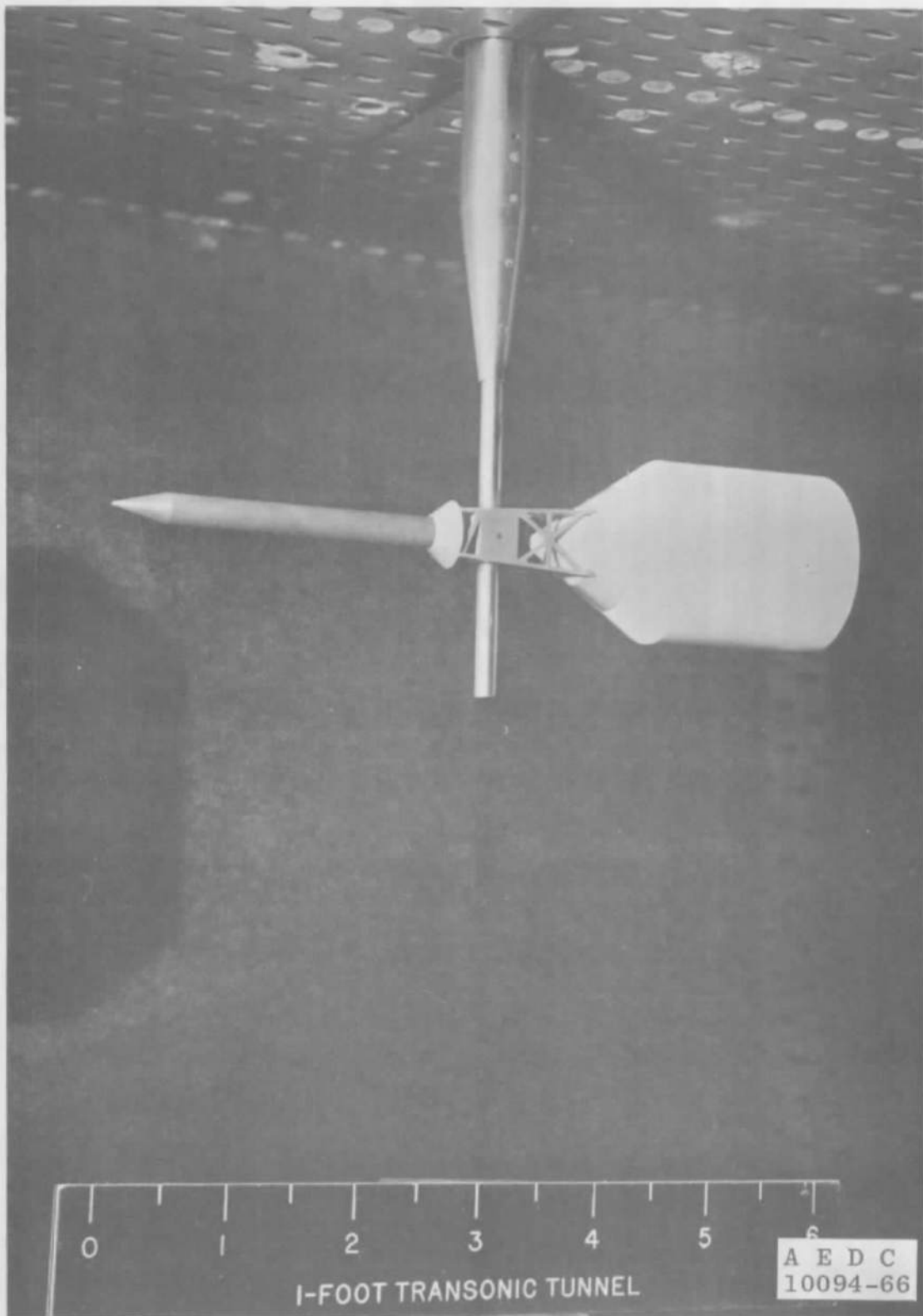


b. Transverse Rod-Supported Model

Fig. 1 Concluded

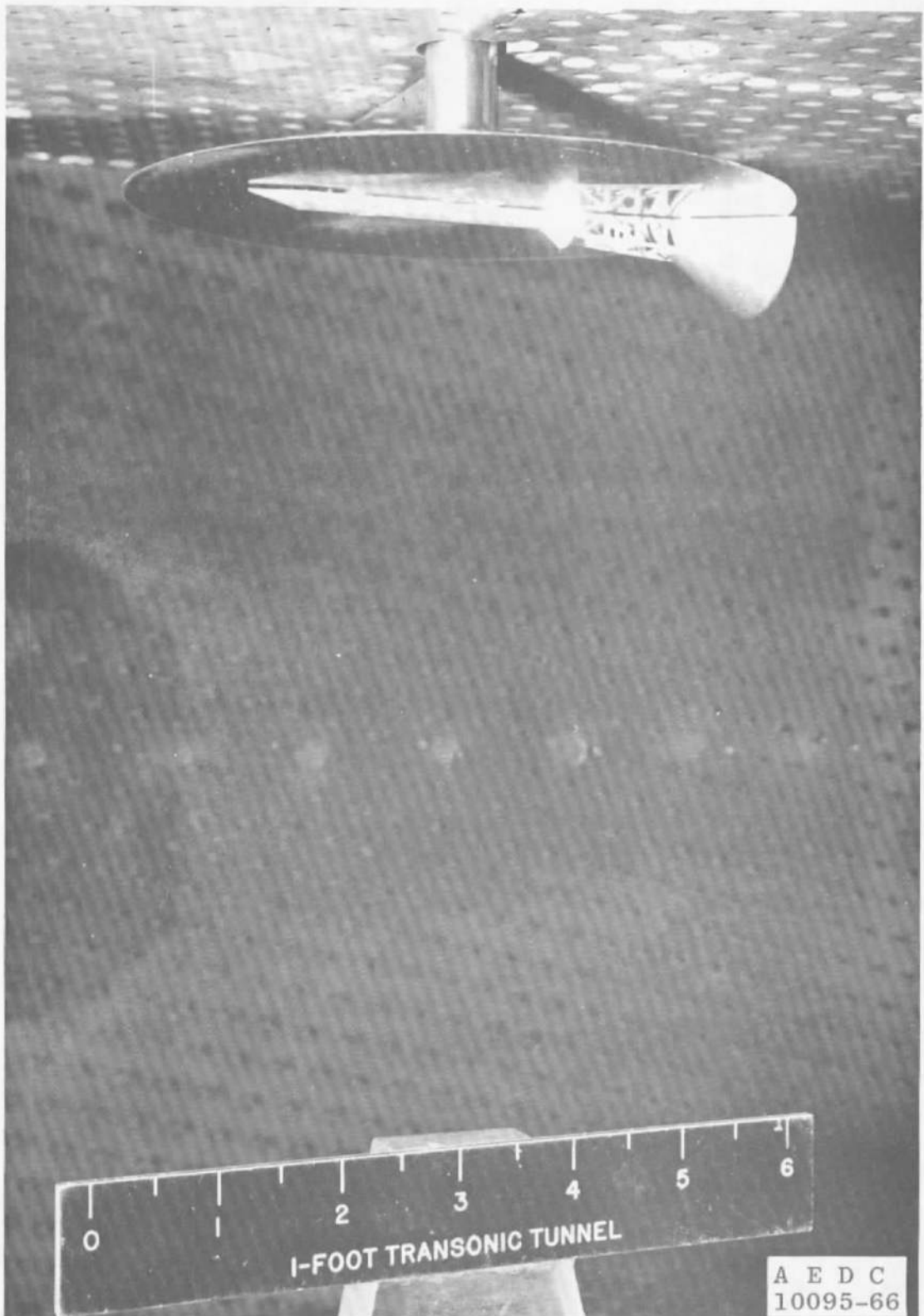


a. Configuration B1DS1-05S, Sting Mounted
Fig. 2 Photographs showing Typical Model Installation and Rotation Centers



b. Configuration B1S1-02R, Transverse Rod Supported

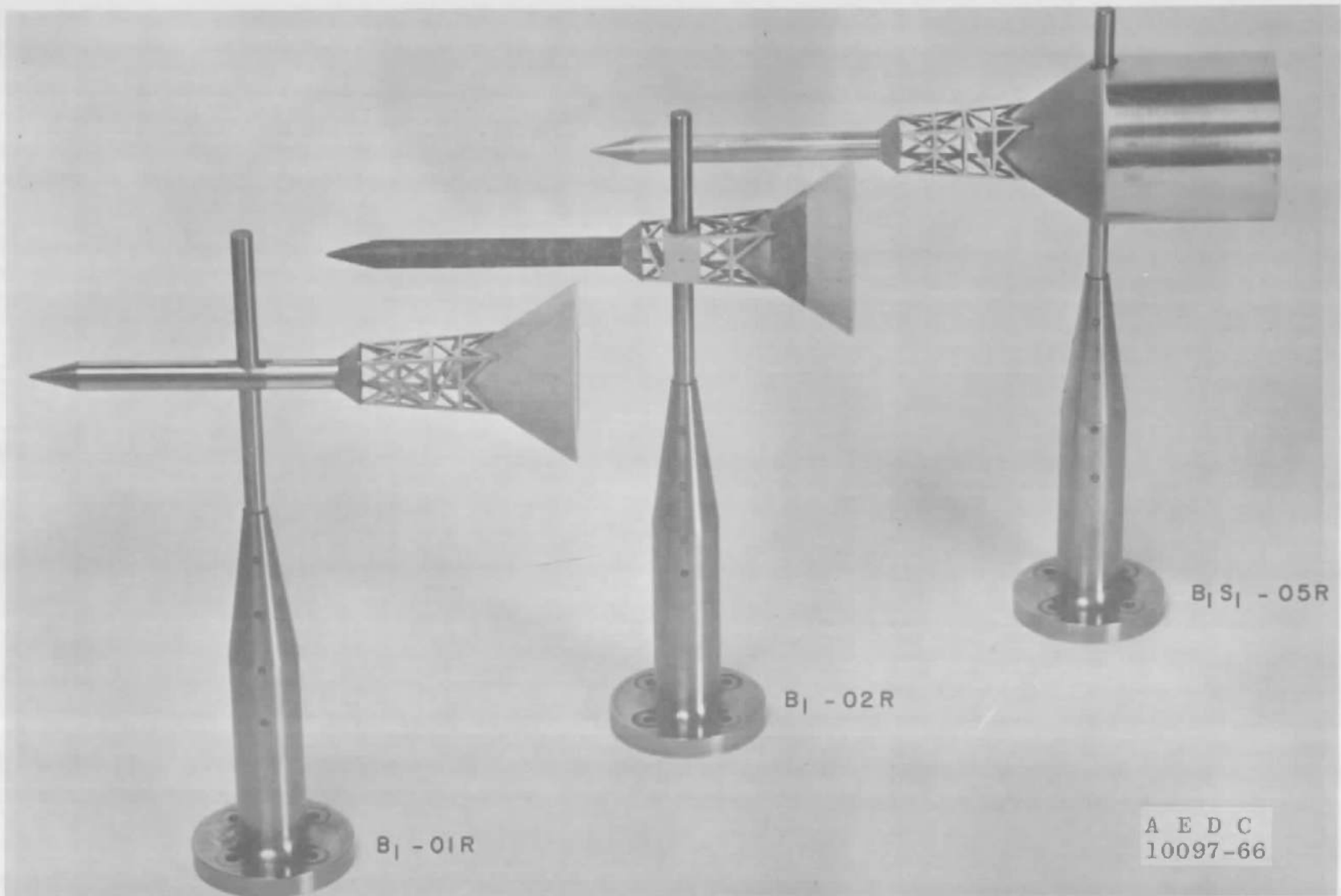
Fig. 2 Continued



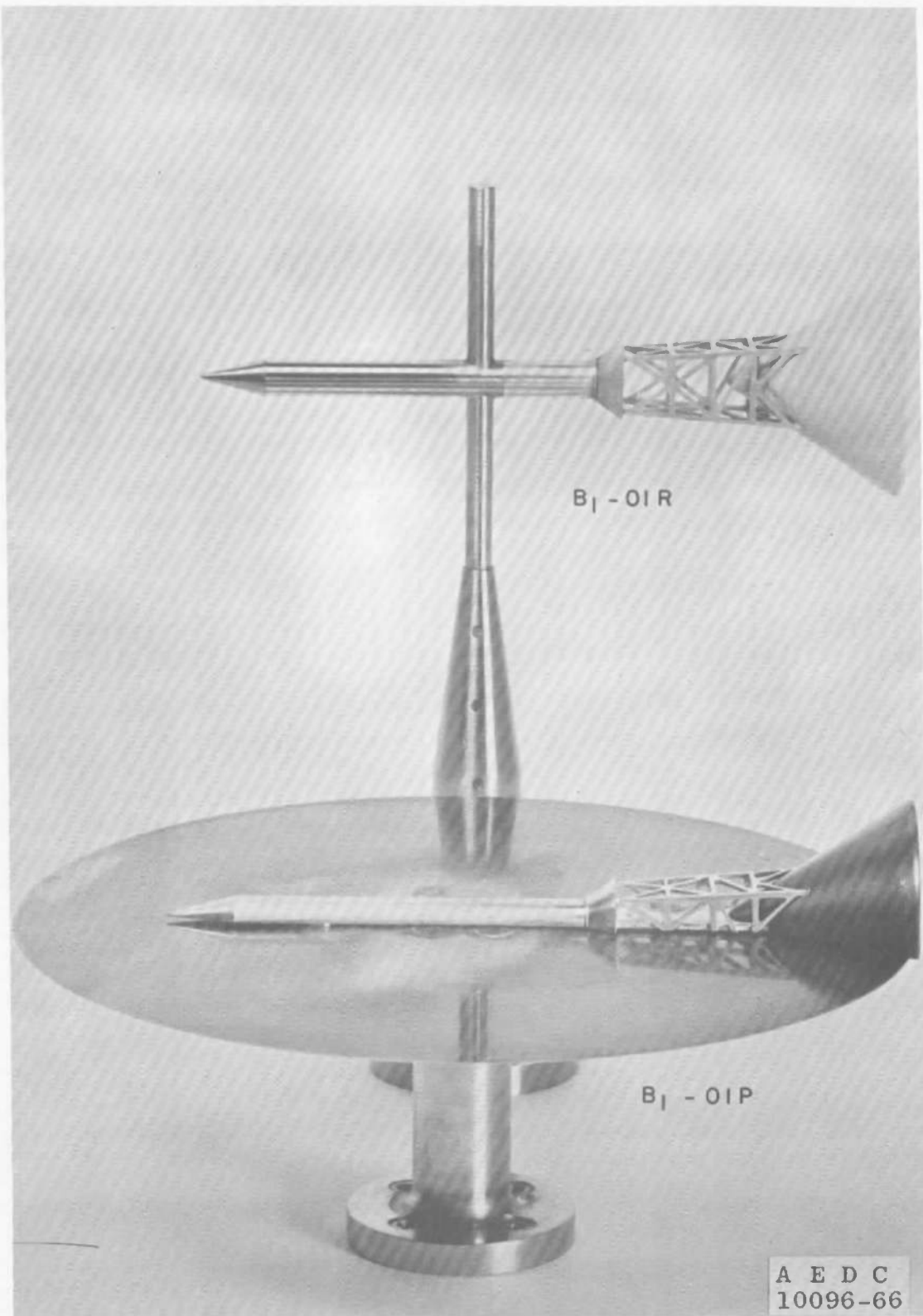
c. Configuration B1-01P, Reflection Plane Mounted

Fig. 2 Continued

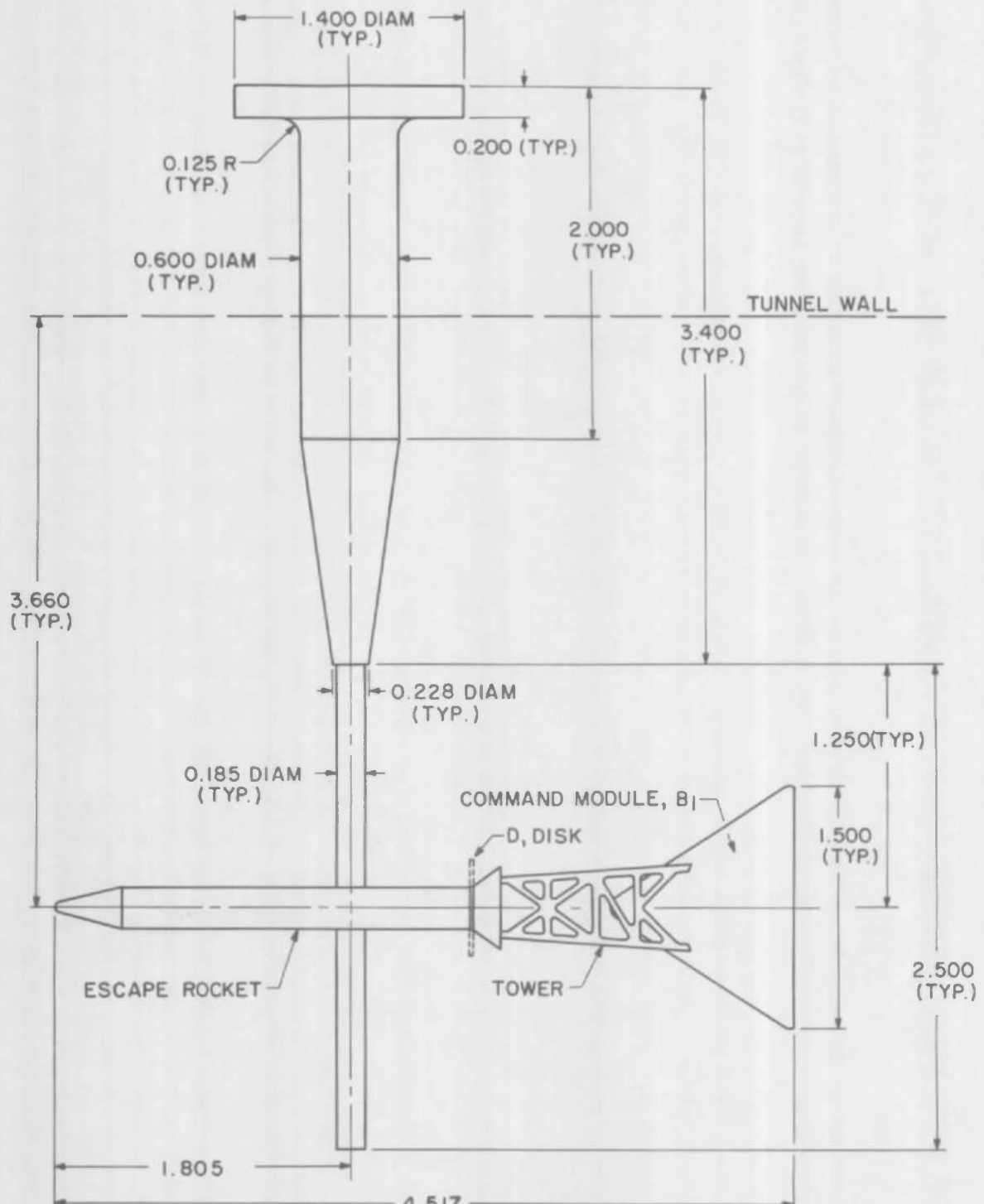
A E D C
10095-66



d. Three Model Rotation Centers, 01, 02, and 05
Fig. 2 Continued



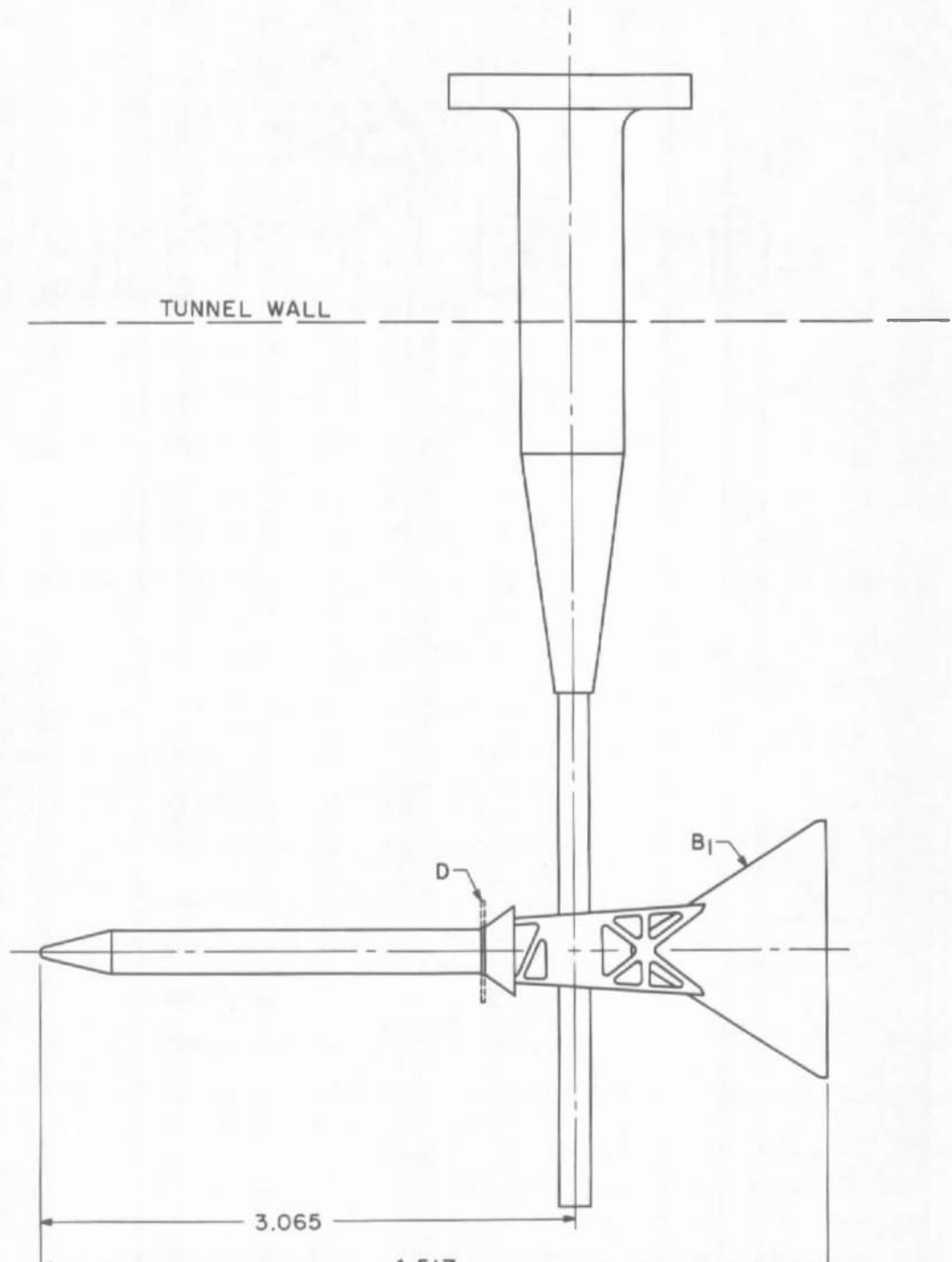
e. Transverse Rod and Reflection Plane Mounting of the B1-01 Configuration
Fig. 2 Concluded



ALL DIMENSIONS IN INCHES

a. Configuration B1-01, (B1D-01)

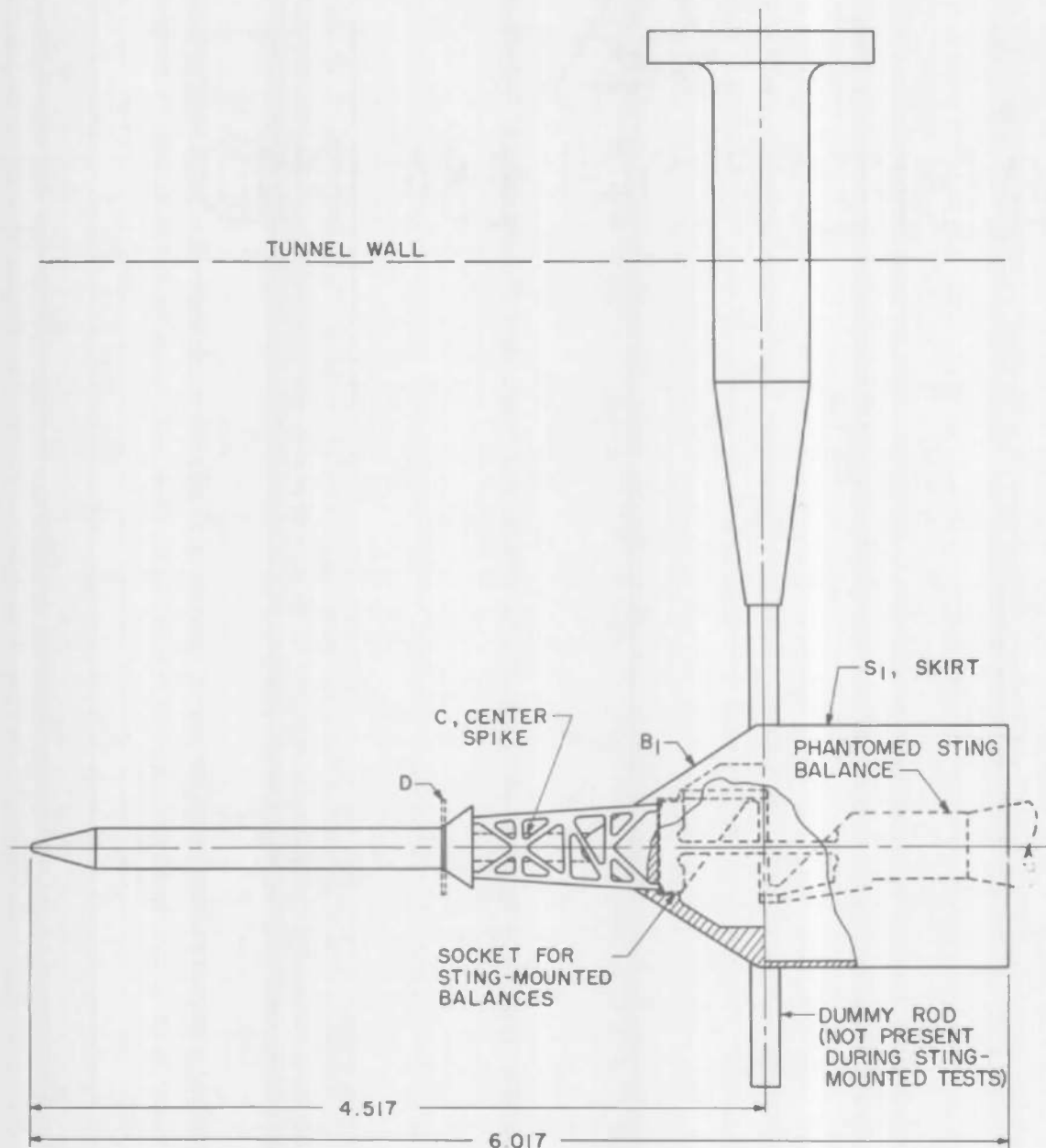
Fig. 3 Model Configuration Drawings



ALL DIMENSIONS IN INCHES

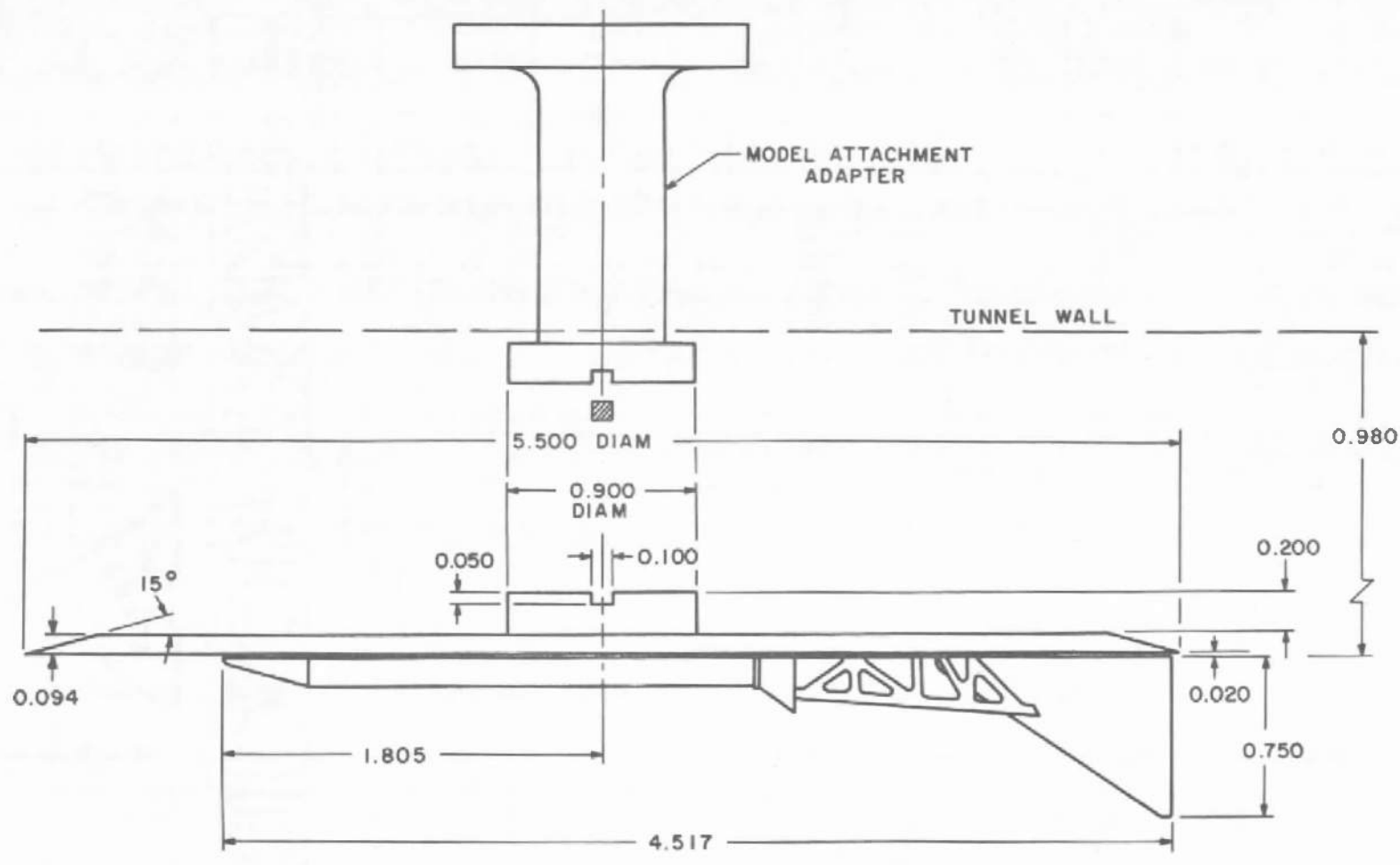
b. Configuration B1-02, (B1D-02)

Fig. 3 Continued



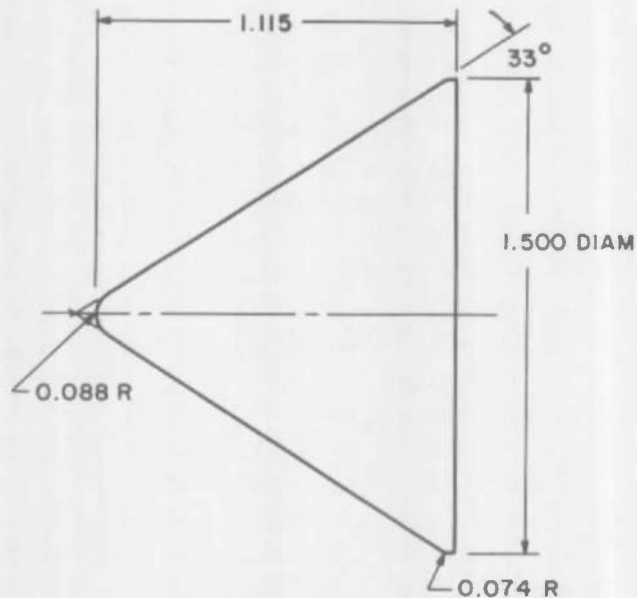
c. Configuration B₁S₁-05 (B₁DS₁-05, B₁CS₁-05)

Fig. 3 Continued

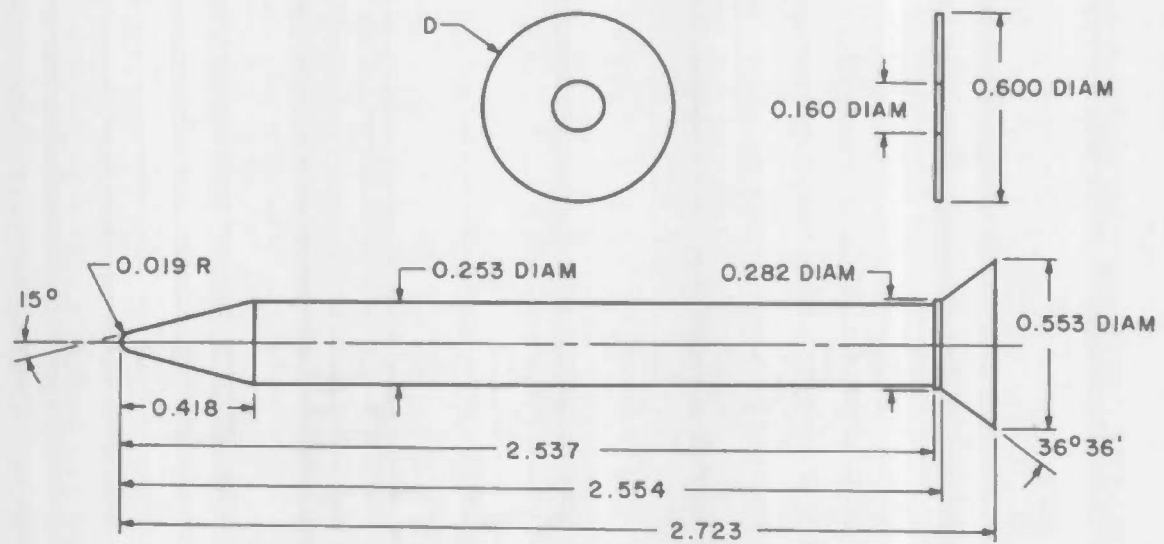


d. Configuration B1-01P

Fig. 3 Continued



B₁ COMMAND MODULE

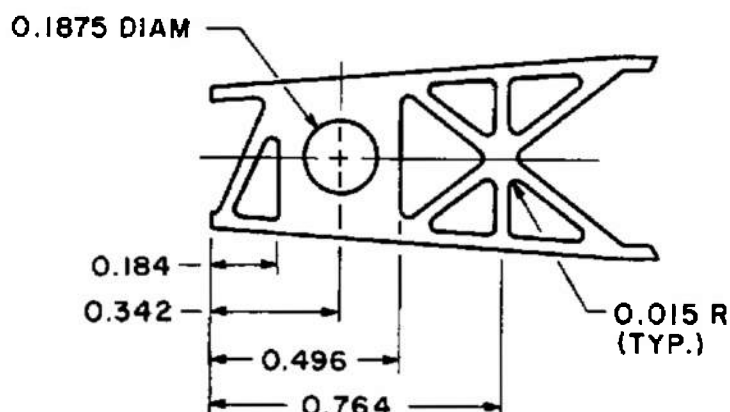
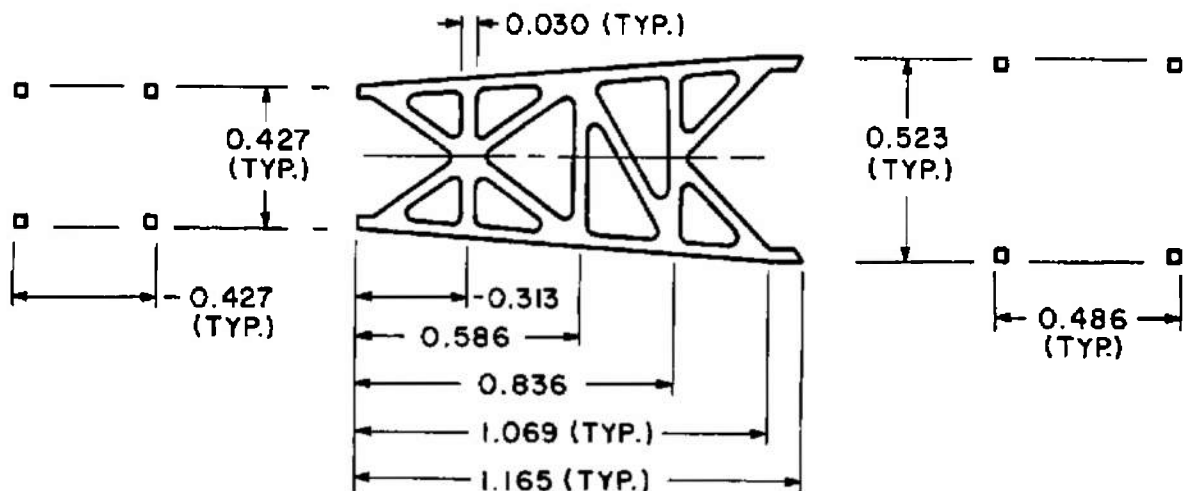


ESCAPE ROCKET

ALL DIMENSIONS IN INCHES

e. Details of B₁ Command Module and Escape Rocket

Fig. 3 Continued

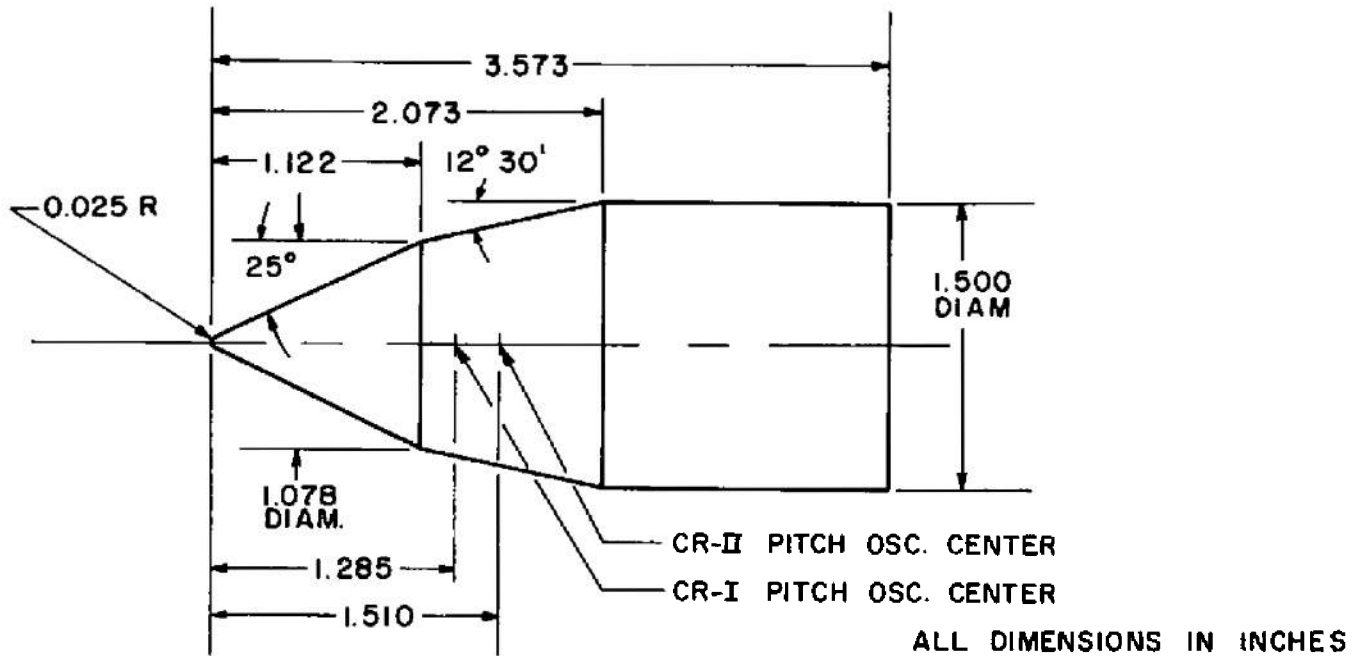


ALL DIMENSIONS IN INCHES

ROCKET TOWER

f. Details of Rocket Tower

Fig. 3 Continued



g. Configuration CR-I and CR-II
Fig. 3 Concluded

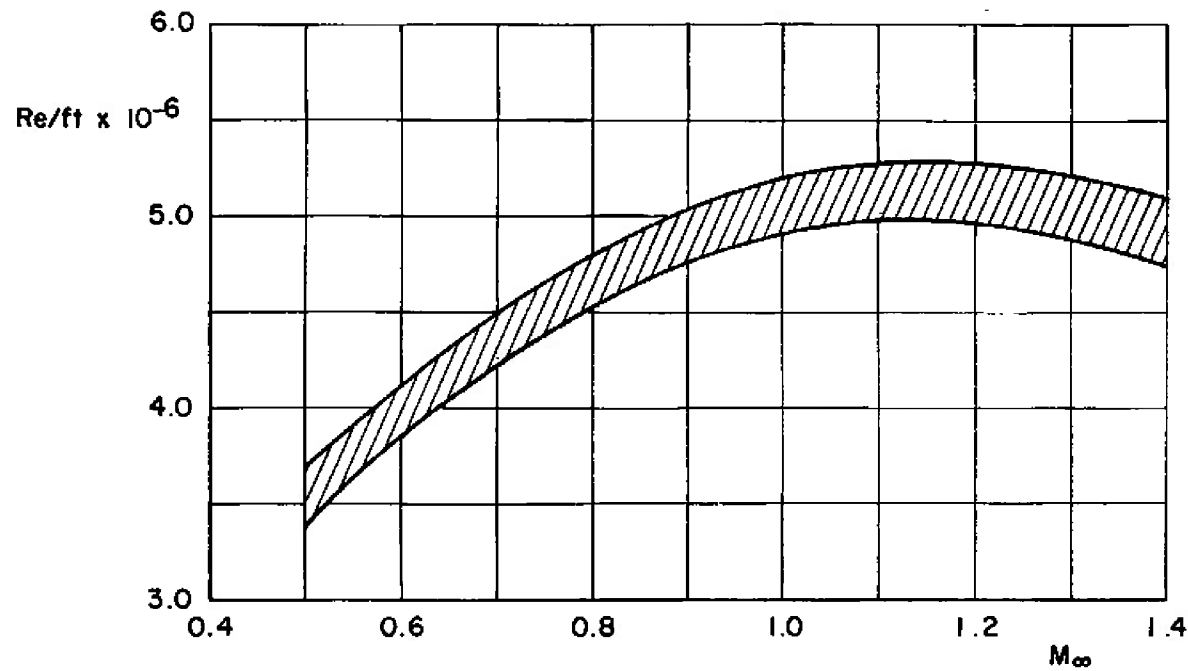


Fig. 4 Reynolds Number Variation with Mach Number

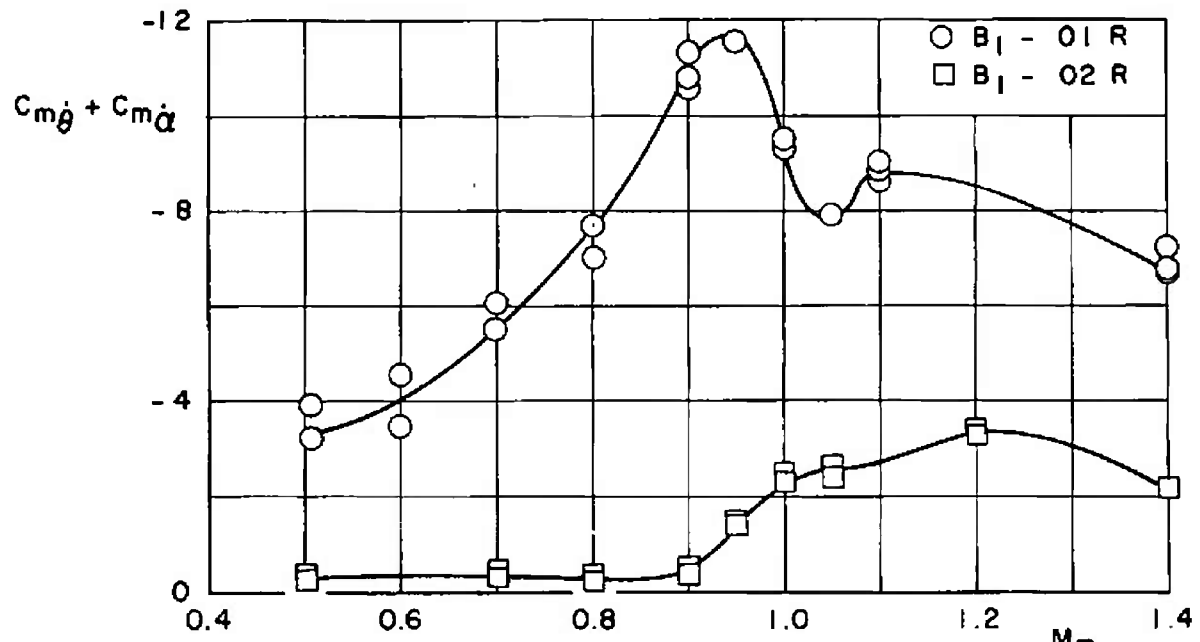
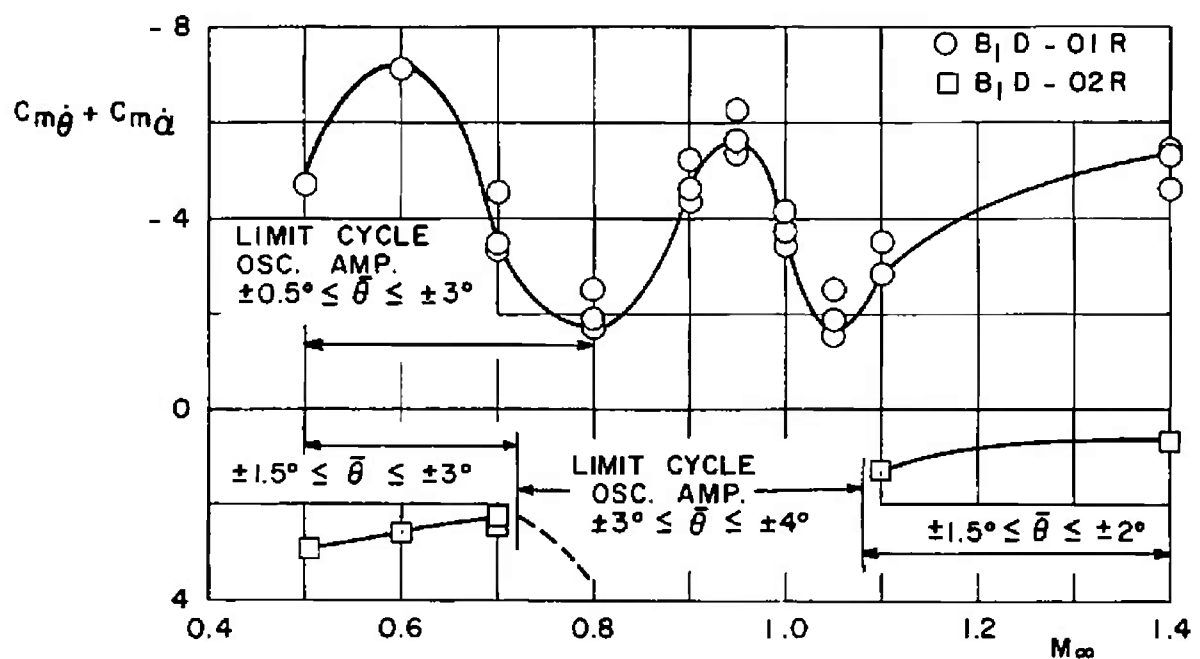
a. Configuration B_1 b. Configuration $B_1 D$

Fig. 5 Apollo-Saturn Model Configurations; Effect of Pitch Oscillation Center on Dynamic Stability Derivatives versus Mach Number, $\alpha = 0$

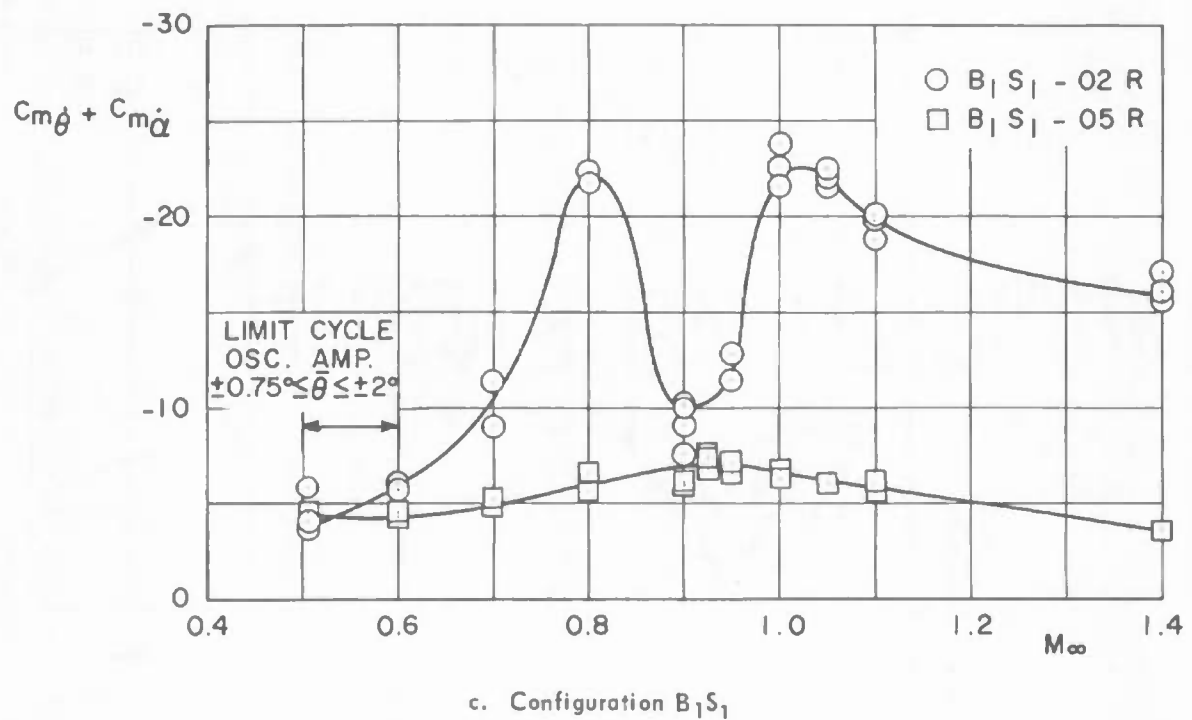
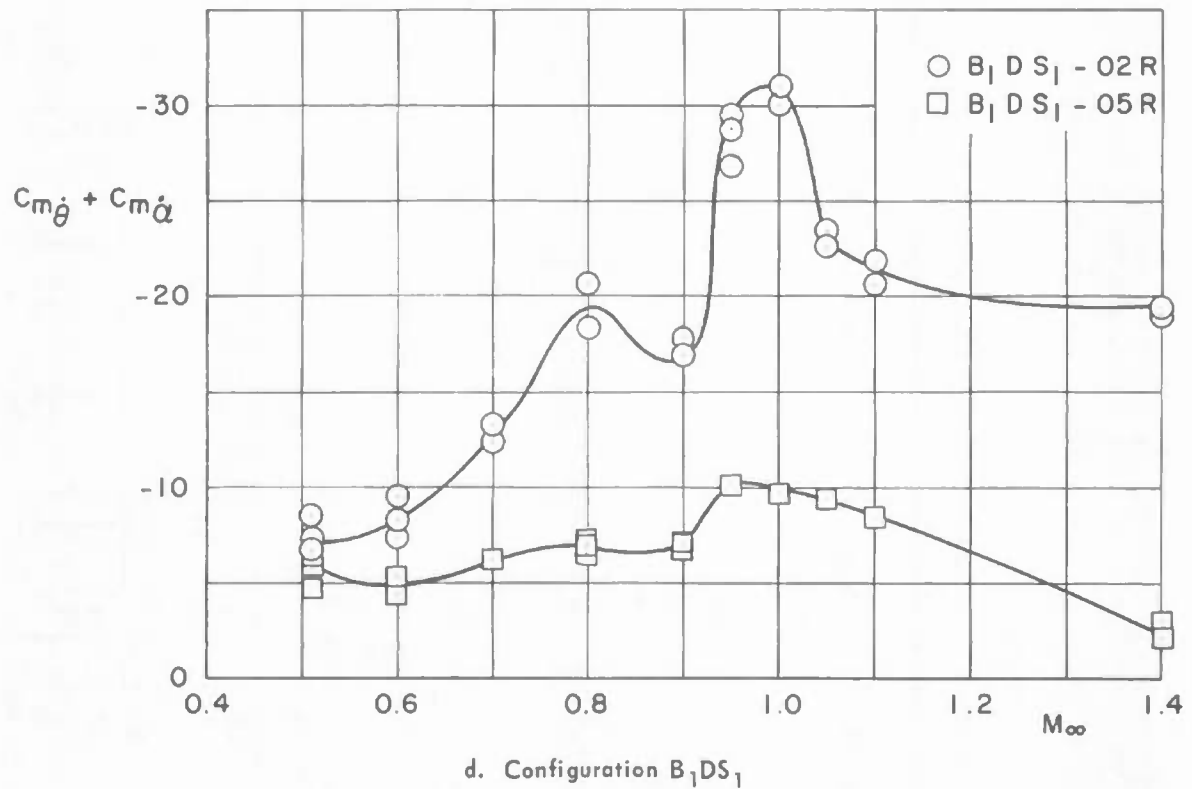
c. Configuration B_1S_1 d. Configuration B_1DS_1

Fig. 5 Concluded

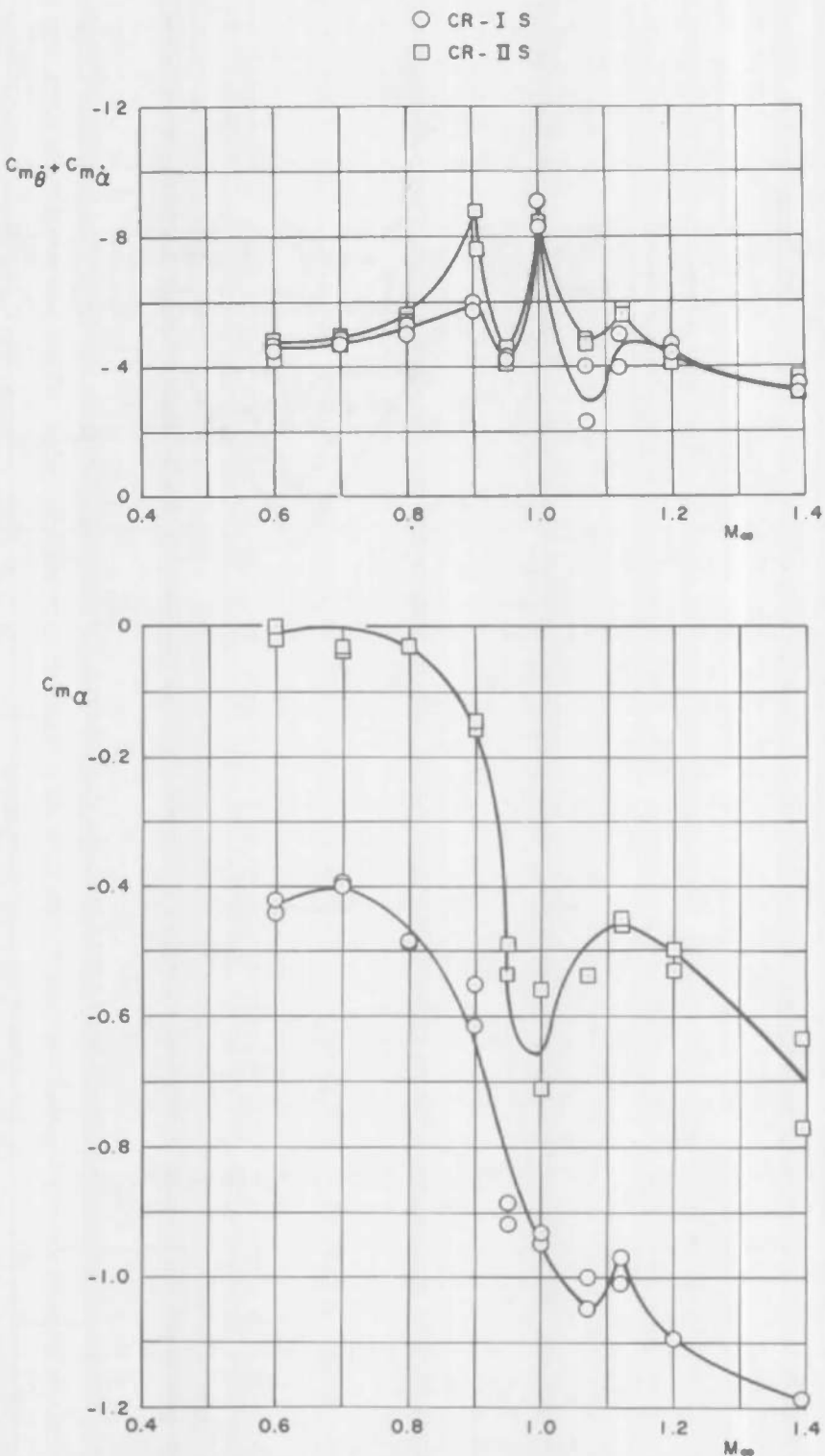


Fig. 6 Saturn-Centaur Model Configurations; Effect of Pitch Oscillation Center on Stability Derivatives versus Mach Number, $\alpha = 0$, Configurations CR-IS and CR-IIS

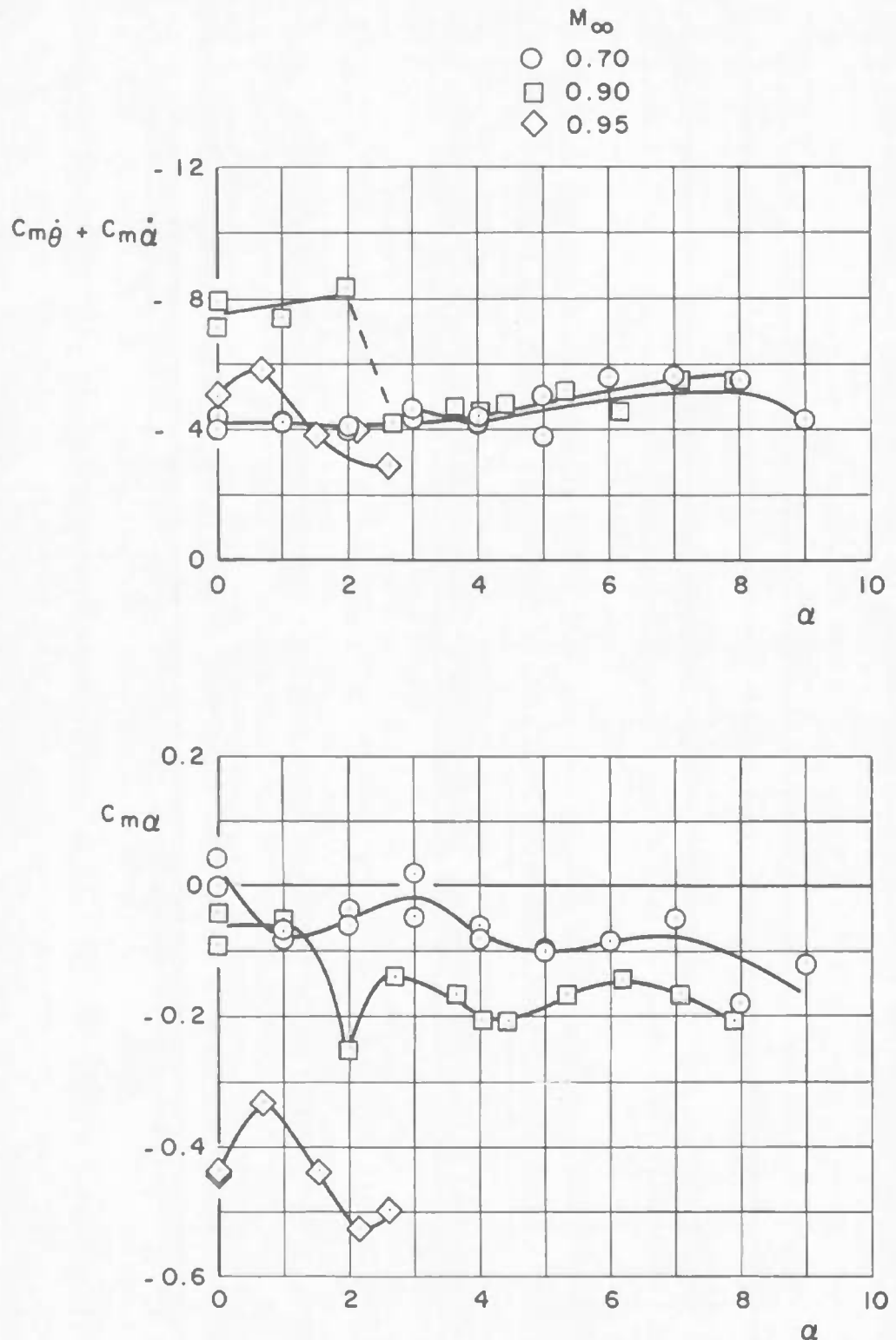


Fig. 7 Saturn-Centaur Model Configuration, Stability Derivatives versus Angle of Attack
 $M_\infty = 0.70, 0.90$, and 0.95 , Configuration CR-IIS

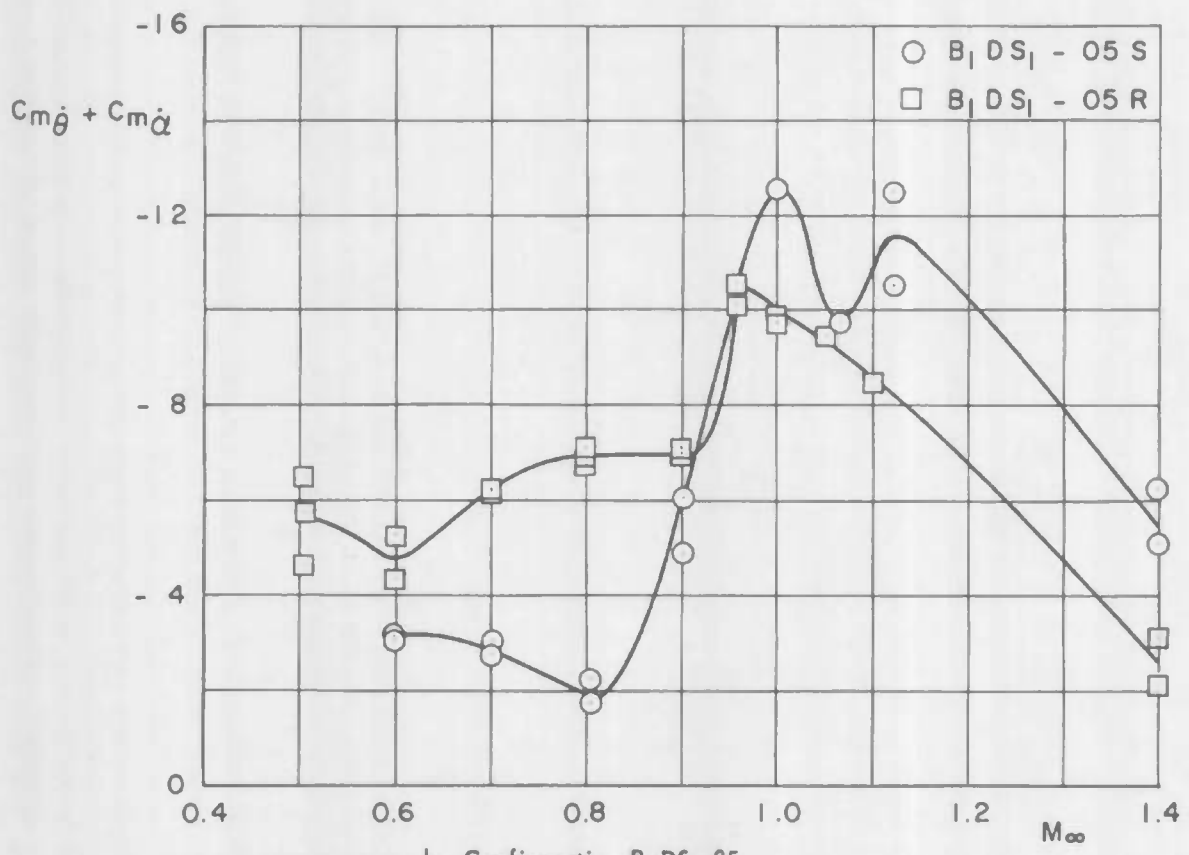
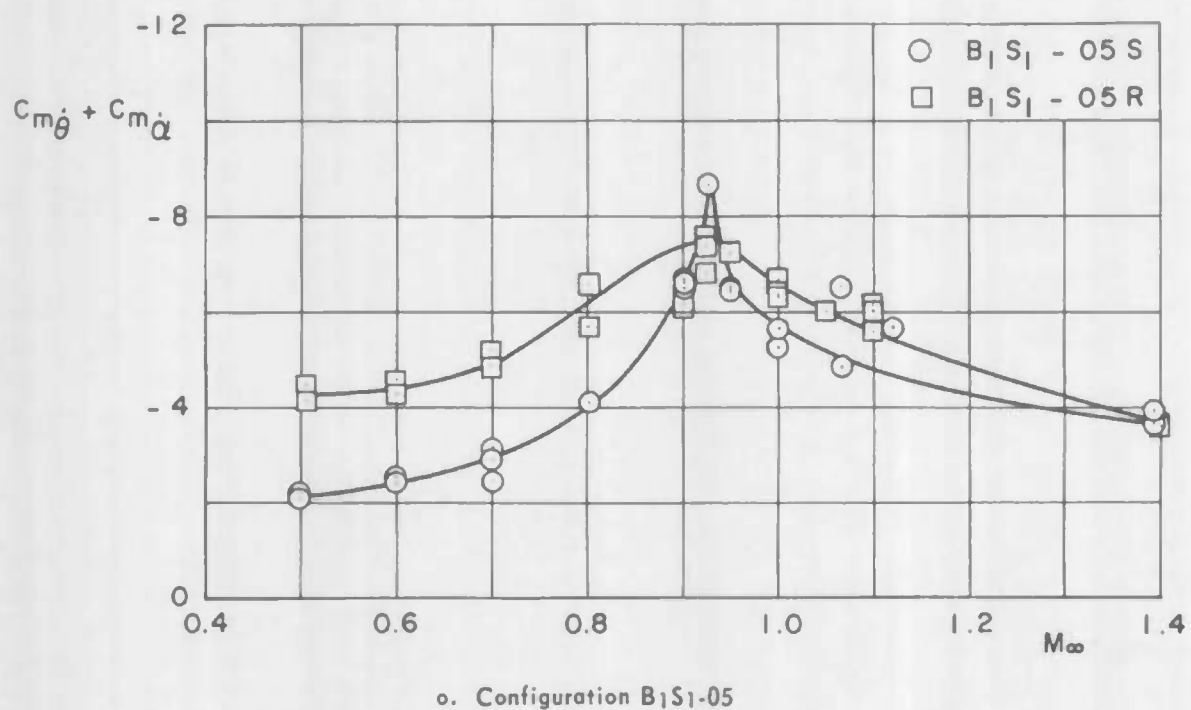
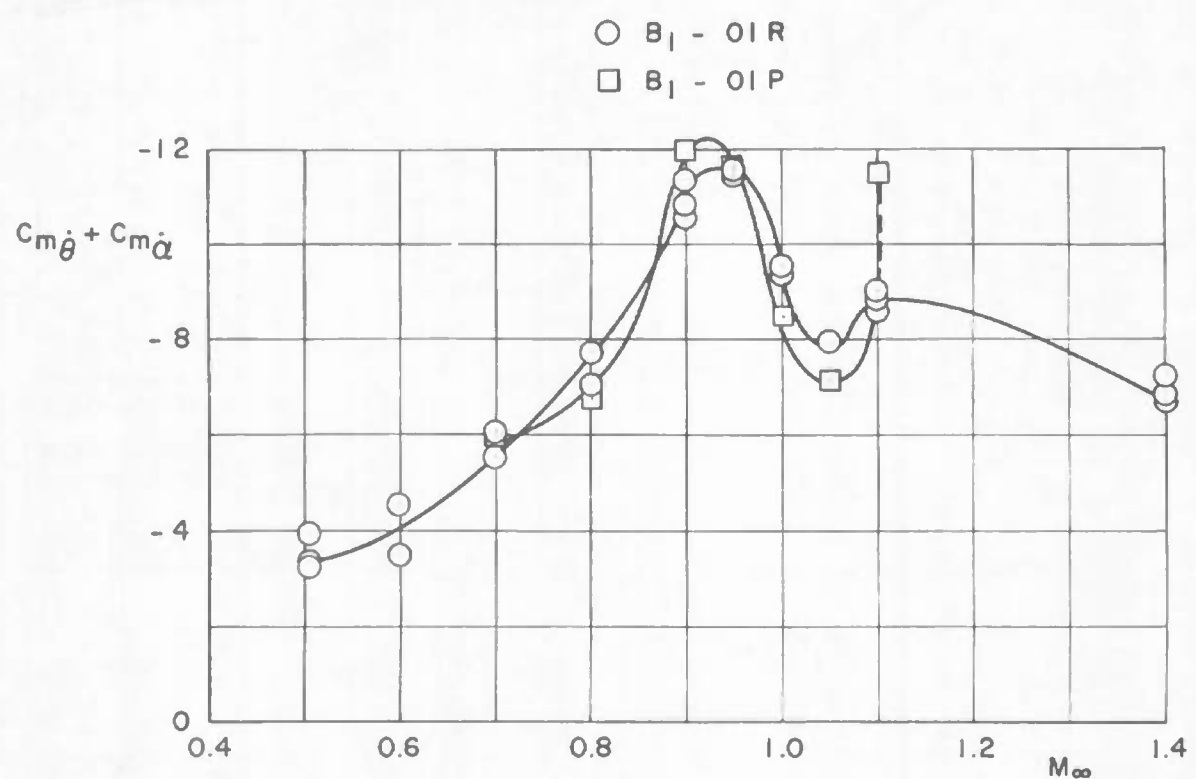


Fig. 8 Dynamic Stability Derivatives versus Mach Number Compared for Different Model Mounting Techniques, $\alpha = 0$



c. Configuration B1-01

Fig. 8 Concluded

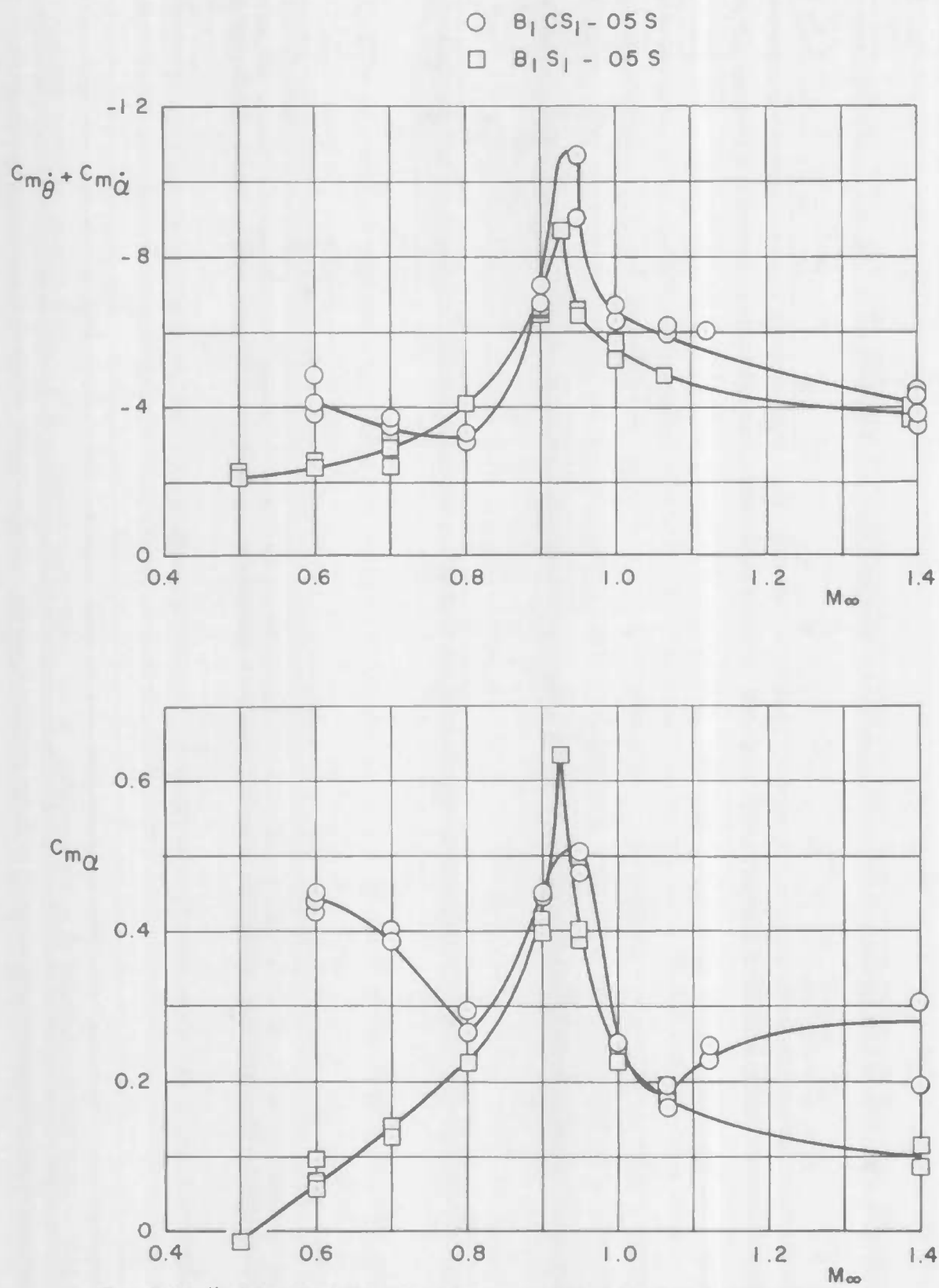
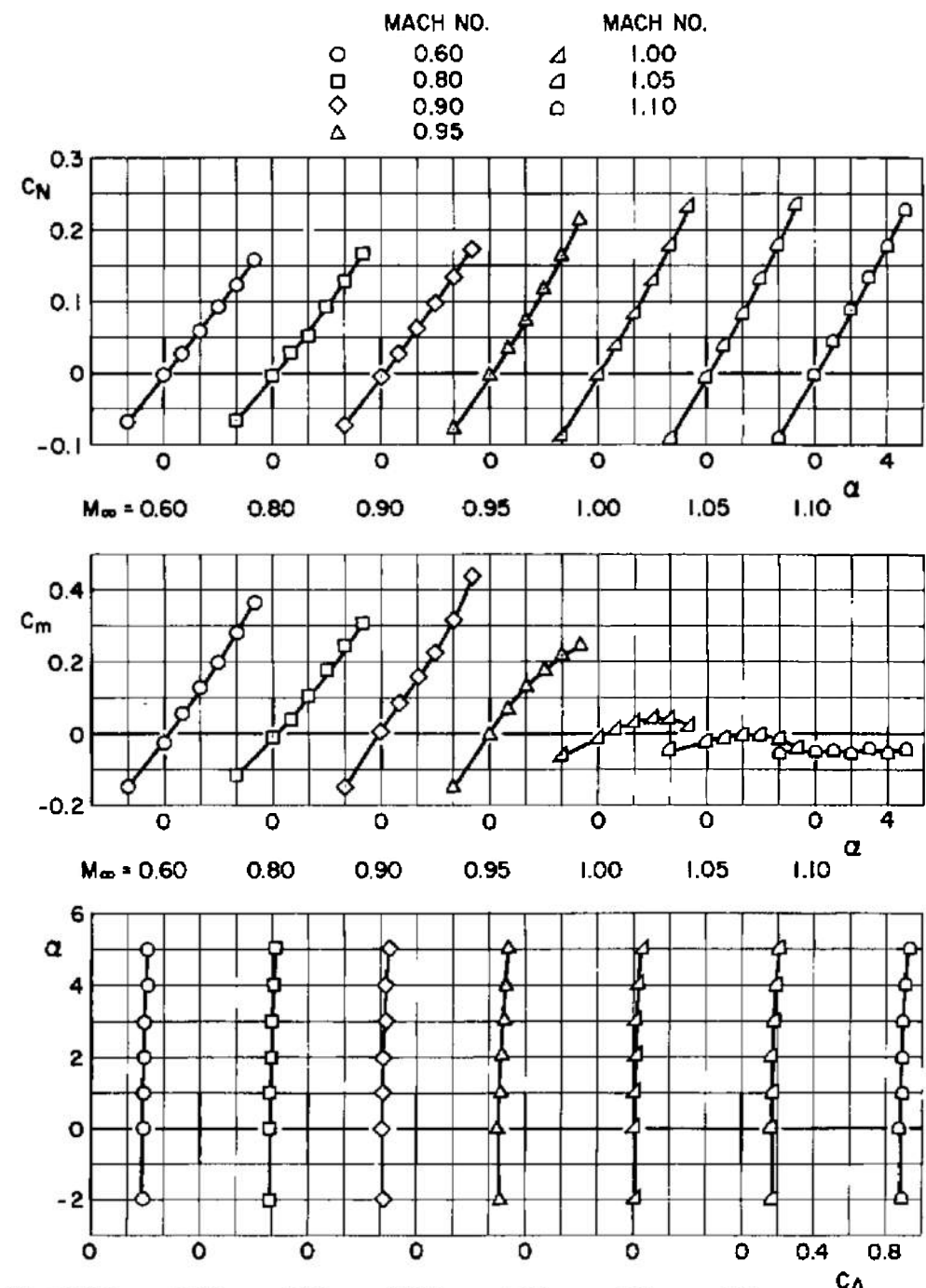
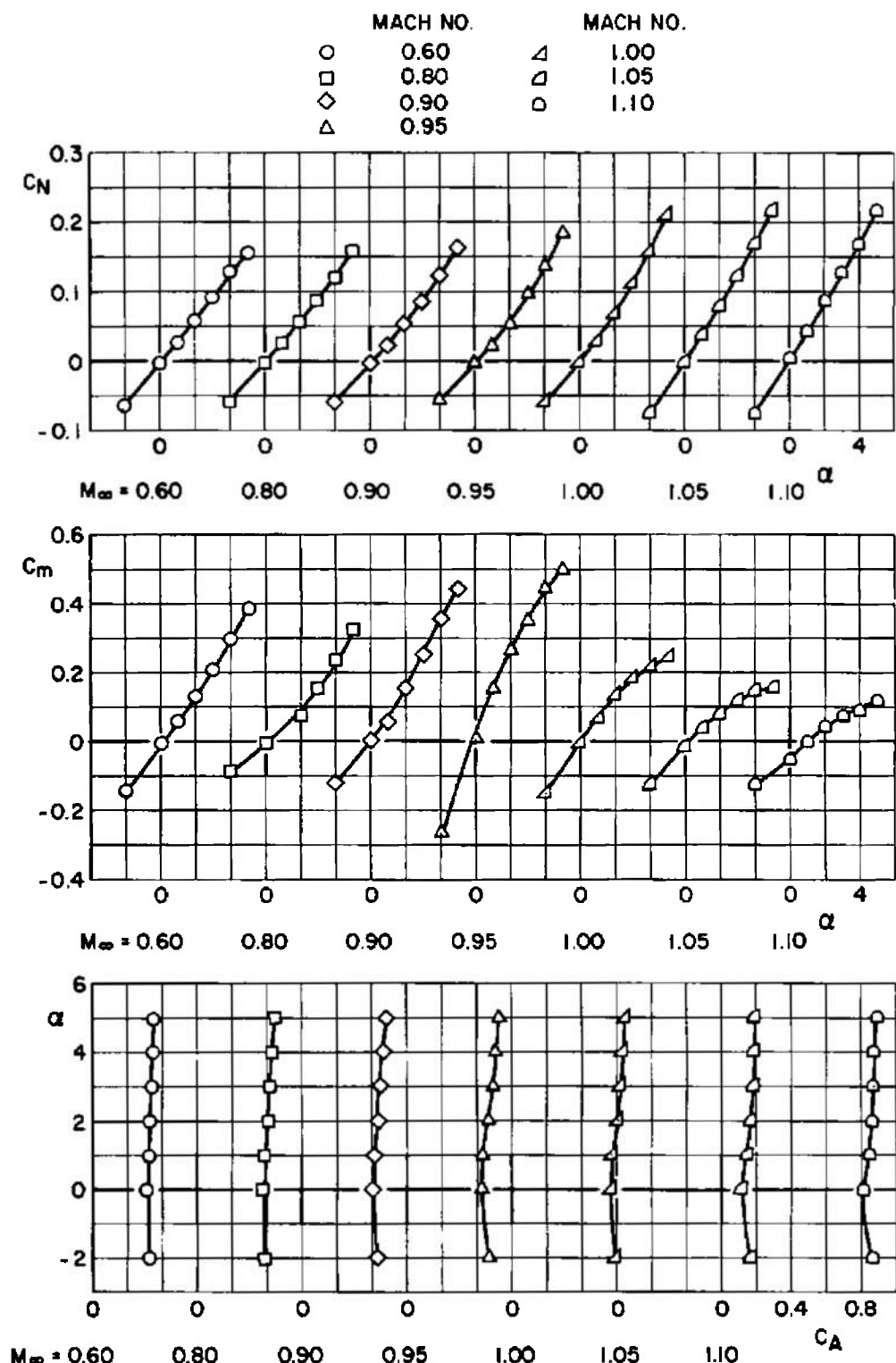


Fig. 9 Apollo-Saturn Stability Derivatives versus Mach Number, Configurations
 B_1B_1-05S and $B_1CS-05S$, $\alpha = 0$



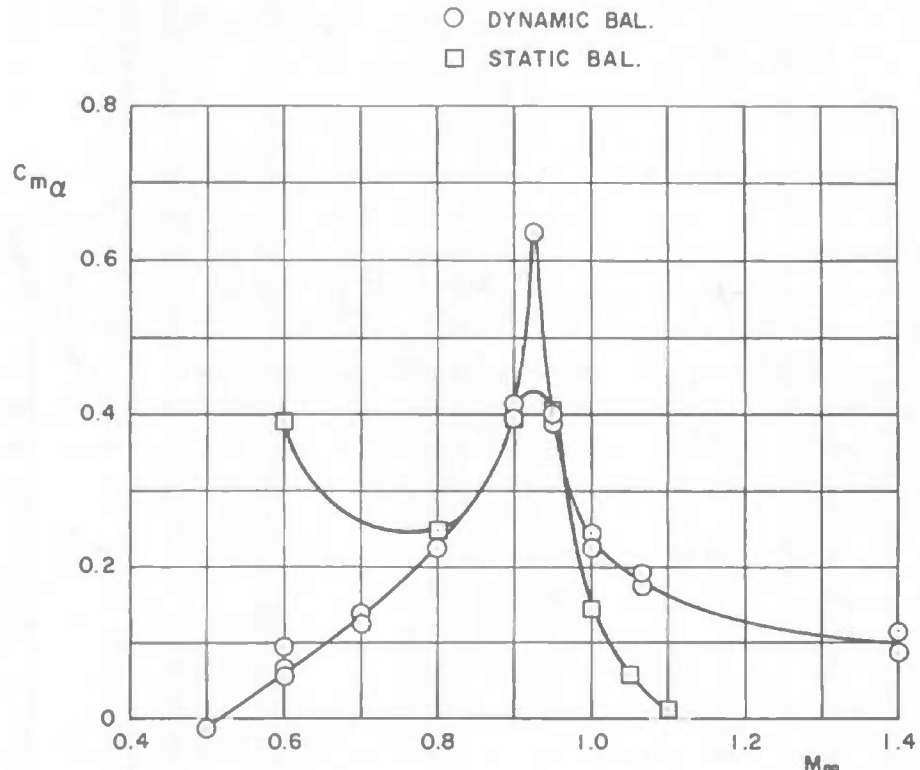
a. Configuration B₁S₂ 055

**Fig. 10 Static Force and Moment Coefficients for Apollo-Saturn Configurations
P+S-055 and P+DS-055**

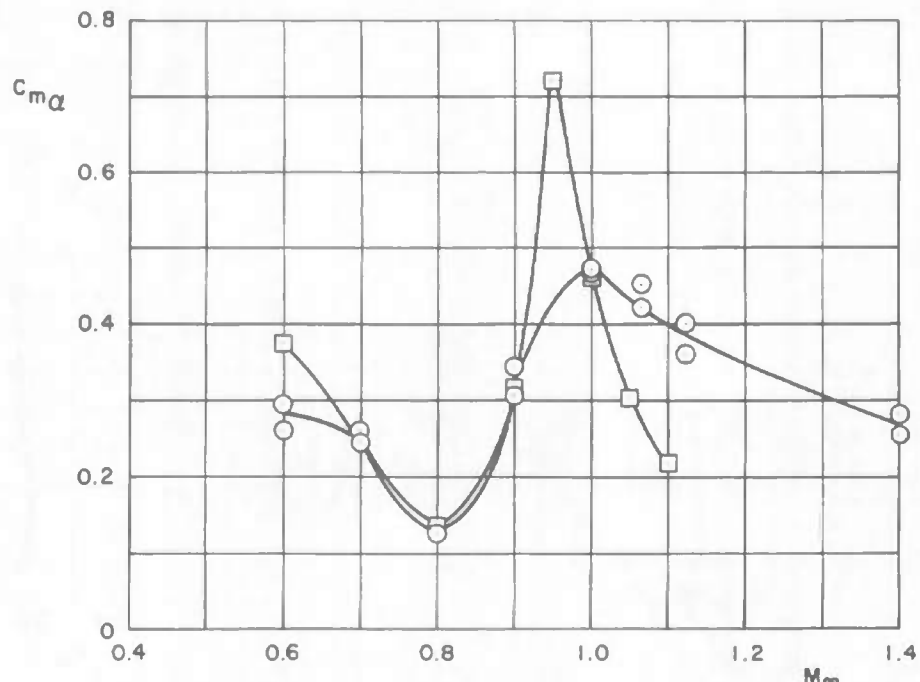


b. Configuration B1DS1-055

Fig. 10 Concluded



a. Configuration B1S1-05S



b. Configuration B1DS1-05S

Fig. 11 Static Stability Derivatives for Apollo-Saturn Configurations B1S1-05S and B1DS1-05S

TABLE I
MODEL DESCRIPTION

<u>Configuration</u>	<u>Pitch Center</u>	<u>Mount</u>	<u>Notation Key</u>	
B ₁	01	R	B ₁	Command Module
B ₁	01	P	D	Disk
B ₁ D	01	R	S ₁	Skirt
B ₁	02	R	C	Center Spike
B ₁ D	02	R	CR	Saturn-Centaur Upper Stage
B ₁ S ₁	02	R	R	Transverse Rod Support Balance
B ₁ DS ₁	02	R	S	Sting Support Balance
B ₁ S ₁	05	S*	P	Reflection Plane Mounted on Transverse Rod Balance
B ₁ S ₁	05	R		
B ₁ DS ₁	05	S*		
B ₁ DS ₁	05	R		
B ₁ CS ₁	05	S		
B ₁ CDS ₁	05	R	NOTE: For static results, 05 indicates moment reference center.	
CR	I	S		
CR	II	S	*Tested both Statically and Dynamically	

REMARKS:

Pitch Center 01 - 1.805 in. Aft of Rocket Nose.

Pitch Center 02 - 3.065 in. Aft of Rocket Nose.

Pitch Center 05 - 4.517 in. Aft of Rocket Nose.

Pitch Center I - 1.285 in. Aft of Nose.

Pitch Center II - 1.510 in. Aft of Nose.

UNCLASSIFIED

Security Classification

DOCUMENT CONTROL DATA - R&D

(Security classification of title, body of abstract and indexing annotation must be entered when the overall report is classified)

1 ORIGINATING ACTIVITY (Corporate author) Arnold Engineering Development Center, ARO, Inc., Operating Contractor, Arnold Air Force Station, Tennessee		2a REPORT SECURITY CLASSIFICATION UNCLASSIFIED
		2b GROUP N/A
3 REPORT TITLE TRANSonic STATIC AND DYNAMIC STABILITY CHARACTERISTICS OF SEVERAL SATURN IB AND V UPPER STAGE CONFIGURATIONS		
4 DESCRIPTIVE NOTES (Type of report and inclusive dates) N/A		
5 AUTHOR(S) (Last name, first name, initial) R. I. Lowndes and T. O. Shadow, ARO, Inc.		
6. REPORT DATE June 1966	7a TOTAL NO OF PAGES 46	7b NO OF REFS 4
8a CONTRACT OR GRANT NO. AF40(600)1200	9a ORIGINATOR'S REPORT NUMBER(S) AEDC-TR-66-125	
b PROJECT NO System 921E	9b OTHER REPORT NO(S) (Any other numbers that may be assigned this report) N/A	
10. AVAILABILITY/LIMITATION NOTICES Qualified users may obtain copies of this report from DDC. Release to foreign nationals or foreign governments must have prior approval of NASA-MSFC.		
11 SUPPLEMENTARY NOTES N/A	12. SPONSORING MILITARY ACTIVITY Marshall Space Flight Center (MSFC), National Aeronau- tics and Space Administration (NASA), Redstone Arsenal, Alabama	
13 ABSTRACT Dynamic stability characteristics of six Apollo-Saturn IB and V and one Saturn-Centaur upper stage model configurations and static stability characteristics of two Apollo-Saturn B and V upper stage model configurations were obtained from $M_{\infty} = 0.50$ to 1.40. The primary test objective was to investigate the changes in dynamic stability characteristics as a function of pitch oscillation center. A secondary objective was to compare three different model mounting techniques - sting, transverse rod, and reflection plane. The static testing resulted from a suspected nonlinear phenomenon observed during the dynamic phase of the test. One model configuration which was stable when the pitch oscillation center was ahead of a separation disk exhibited limit cycle oscillations when the pitch oscillation center was located aft of the disk.		
<p style="text-align: right;">This document has been approved for public release by distribution is unlimited. For A. J. Letter dated 15 June, 1973</p>		

UNCLASSIFIED

Security Classification

14	KEY WORDS	LINK A		LINK B		LINK C	
		ROLE	WT	ROLE	WT	ROLE	WT
2	Project Centaur						
3	Project Saturn IB and V						
	transonic flow						
	static stability						
	dynamics stability						
1.	Space vehicles -- Stability						
4 Transonic flow						

INSTRUCTIONS

1. ORIGINATING ACTIVITY: Enter the name and address of the contractor, subcontractor, grantee, Department of Defense activity or other organization (corporate author) issuing the report.

2a. REPORT SECURITY CLASSIFICATION: Enter the overall security classification of the report. Indicate whether "Restricted Data" is included. Marking is to be in accordance with appropriate security regulations.

2b. GROUP: Automatic downgrading is specified in DoD Directive 5200.10 and Armed Forces Industrial Manual. Enter the group number. Also, when applicable, show that optional markings have been used for Group 3 and Group 4 as authorized.

3. REPORT TITLE: Enter the complete report title in all capital letters. Titles in all cases should be unclassified. If a meaningful title cannot be selected without classification, show title classification in all capitals in parenthesis immediately following the title.

4. DESCRIPTIVE NOTES: If appropriate, enter the type of report, e.g., interim, progress, summary, annual, or final. Give the inclusive dates when a specific reporting period is covered.

5. AUTHOR(S): Enter the name(s) of author(s) as shown on or in the report. Enter last name, first name, middle initial. If military, show rank and branch of service. The name of the principal author is an absolute minimum requirement.

6. REPORT DATE: Enter the date of the report as day, month, year, or month, year. If more than one date appears on the report, use date of publication.

7a. TOTAL NUMBER OF PAGES: The total page count should follow normal pagination procedures, i.e., enter the number of pages containing information.

7b. NUMBER OF REFERENCES: Enter the total number of references cited in the report.

8a. CONTRACT OR GRANT NUMBER: If appropriate, enter the applicable number of the contract or grant under which the report was written.

8b. & 8d. PROJECT NUMBER: Enter the appropriate military department identification, such as project number, subproject number, system numbers, task number, etc.

9a. ORIGINATOR'S REPORT NUMBER(S): Enter the official report number by which the document will be identified and controlled by the originating activity. This number must be unique to this report.

9b. OTHER REPORT NUMBER(S): If the report has been assigned any other report numbers (either by the originator or by the sponsor), also enter this number(s).

10. AVAILABILITY/LIMITATION NOTICES: Enter any limitations on further dissemination of the report, other than those

imposed by security classification, using standard statements such as:

- (1) "Qualified requesters may obtain copies of this report from DDC."
- (2) "Foreign announcement and dissemination of this report by DDC is not authorized."
- (3) "U. S. Government agencies may obtain copies of this report directly from DDC. Other qualified DDC users shall request through ."
- (4) "U. S. military agencies may obtain copies of this report directly from DDC. Other qualified users shall request through ."
- (5) "All distribution of this report is controlled. Qualified DDC users shall request through ."

If the report has been furnished to the Office of Technical Services, Department of Commerce, for sale to the public, indicate this fact and enter the price, if known.

11. SUPPLEMENTARY NOTES: Use for additional explanatory notes.

12. SPONSORING MILITARY ACTIVITY: Enter the name of the departmental project office or laboratory sponsoring (paying for) the research and development. Include address.

13. ABSTRACT: Enter an abstract giving a brief and factual summary of the document indicative of the report, even though it may also appear elsewhere in the body of the technical report. If additional space is required, a continuation sheet shall be attached.

It is highly desirable that the abstract of classified reports be unclassified. Each paragraph of the abstract shall end with an indication of the military security classification of the information in the paragraph, represented as (TS), (S), (C), or (U).

There is no limitation on the length of the abstract. However, the suggested length is from 150 to 225 words.

14. KEY WORDS: Key words are technically meaningful terms or short phrases that characterize a report and may be used as index entries for cataloging the report. Key words must be selected so that no security classification is required. Identifiers, such as equipment model designation, trade name, military project code name, geographic location, may be used as key words but will be followed by an indication of technical context. The assignment of links, rules, and weights is optional.

UNCLASSIFIED

Security Classification